

STUDY FOR THE INDICIAL LOAD EFFECTS ON MULTISTAGE SPACE VEHICLE SYSTEMS

Linearized Indicial Aerodynamic Forces on Bodies of
Revolution in Supersonic Flow

ANNUAL SUMMARY REPORT - Volume I
21 June 1963 - 20 August 1964

Contract No. NAS8-11012
Control No. TP3-81150 & S-1 (1F)
CPB 16-609-63 & S-1

MRI Project No. 2715-P

FACILITY FORM 502

N65 21720	
(ACCESSION NUMBER)	(THRU)
93	1
(PAGES)	(CODE)
CP 6.2/99	01
(NASA CR OR TMX OR AD NUMBER)	(CATEGORY)

For

National Aeronautics and Space Administration
Procurement and Contracts Office
George C. Marshall Space Flight Center
Huntsville, Alabama 35812
Attn: Procurement and Contracts Office, M-P&C-MEA



MIDWEST RESE

425 VOLKER BOULEVARD/KANSAS CITY, N

GPO PRICE \$ _____

OTS PRICE(S) \$ _____

Hard copy (HC) 3.60

Microfiche (MF) .25

STUDY FOR THE INDICIAL LOAD EFFECTS ON MULTISTAGE
SPACE VEHICLE SYSTEMS

Linearized Indicial Aerodynamic Forces on Bodies of
Revolution in Supersonic Flow

by

William D. Glauz

ANNUAL SUMMARY REPORT - Volume I
21 June 1963 - 20 August 1964

Contract No. NAS8-11012
Control No. TP3-81150 & S-1 (1F)
CPB 16-609-63 & S-1

MRI Project No. 2715-P

For

National Aeronautics and Space Administration
Procurement and Contracts Office
George C. Marshall Space Flight Center
Huntsville, Alabama 35812
Attn: Procurement and Contracts Office, M-P&C-MEA



MIDWEST RESEARCH INSTITUTE

425 VOLKER BOULEVARD/KANSAS CITY, MISSOURI 64110/AC 816 LO 1-0202

PREFACE

The work reported here is Part I of a project performed for the George C. Marshall Space Flight Center under Contract No. NAS8-11012. The project benefited greatly from the suggestions of Dr. Max Platzter, the technical administrator.

The major part of the analysis was performed by Dr. William D. Glauz in the Mathematical Analysis Section. Mr. A. D. St. John was project leader. The assistance of Dr. R. R. Reed, Dr. R. O. Stearman, Mr. J. E. Yates, and Mrs. W. T. Chinnery was of great value, especially in several of the appendices.

Approved for:

MIDWEST RESEARCH INSTITUTE



Sheldon L. Levy, Director
Mathematics and Physics Division

21 August 1964

TABLE OF CONTENTS

	<u>Page No.</u>
Notation	v
Abstract	1
I. Introduction	2
II. Summary	2
III. General Formulation of the Problem	3
IV. A Brief Review of the Literature.	4
V. Derivation of a Class of Solutions of Equation (3.1)	6
VI. Transient Source and Doublet Solutions	14
VII. The Gust Doublet Solution for a Cone	23
VIII. Generalized Force Coefficients	34
IX. Application of the Gust Doublet to Cone-Cylinder Bodies	42
X. Conclusions and Recommendations	46
Bibliography	49
Appendix A - Review of the Karman-Moore and Tsien Theories	52
Appendix B - The use of Surface Source Distributions	56
Appendix C - Application of Bond-Packard Theory	68
Appendix D - A Numerical Approach to the Indicial Aerodynamics	72
Appendix E - The Nonlinear Pressure Coefficient and Related Coefficients	77

TABLE OF CONTENTS (Concluded)

List of Figures

<u>Figure No.</u>	<u>Title</u>	<u>Page No.</u>
1	Regions of Influence Determined by Eq. (5.8) or (5.9) . .	10
2	Regions of Influence of Moving Point Source	17
3	Regions of Integration for Eq. (6.11)	19
4	Regions of Influence Showing C^* and D^*	22
5	Relative Error in Boundary Condition	29
6	Regions of Influence for Various Cones	29
7	Growth of Lift for $MR' = 0.3$	33
8	Steady-State Lift Coefficients	33
9	General Gust Doublet	35
10	Regions of Integration	43
11	Control Points	53
12	Notation for Appendix B	56
13	Location of Doublet Distributions	73
14	Lift Coefficient, Numerical	76
15	Steady-State Lift Coefficient for $M = 1.5$ (Nonlinear) . .	84
16	Steady-State Lift Coefficient for $M = 2.0$ (Nonlinear) . .	84
17	Growth of Lift for $M = 2.0$, $R' = 0.15$ (Nonlinear)	86

List of Tables

<u>Table No.</u>	<u>Title</u>	<u>Page No.</u>
I	Limits for Force Integrals	45
II	Method of Determining A_{mn}	74
III	A_{mn} Values	75

NOTATION

A_{mn}	= strength of a gust doublet.
A, B, C, D, E	= regions defined by Fig. 9.
a	= speed of sound in the undisturbed fluid.
B_k	= source strength.
C_B	= bending moment coefficient.
C_L	= lift (normal force) coefficient.
C_M	= moment coefficient.
C_P	= pressure coefficient.
C_{F_l}	= generalized force coefficient.
f	= an arbitrary function, determined so as to satisfy a boundary condition.
$H(z)$	= unit step function, = 1 if $z \geq 0$ and zero otherwise.
I_n	= modified Bessel function of the first kind, order n .
i	= $\sqrt{-1}$.
K_n	= modified Bessel function of the second kind, order n .
L	= length of body, or Laplace transform.
M	= Mach number, U/a .
P	= r -intercept of straight line in x - r plane, or a point on the body surface.
p	= pressure, or transform variable corresponding to x .
$R(x)$	= equation of the body surface.
r	= radial coordinate.

r_s = spherical radius, $= \sqrt{r^2 + x^2}$.
 S = base area of body.
 s = transform variable corresponding to t or τ .
 T_m = $t - t_m$.
 t = time.
 t_m = the m^{th} time at which a gust doublet starts.
 U = upstream velocity.
 u = axial velocity or perturbation.
 V = strength of an elementary point source.
 v = radial component of velocity.
 v_o = velocity of the side gust.
 W = downwash.
 w = tangential (angular) component of velocity.
 X_n = $x - \xi_n$.
 x = axial coordinate, measured from nose of body.
 α = MR' .
 β = $\sqrt{M^2 - 1}$.
 Γ = Gamma function.
 γ = PR'
 δ = Dirac delta (unit impulse) function, or slenderness ratio.
 θ = angular coordinate.
 ξ = axial coordinate, or location of a point on the x-axis.
 ξ_n = location of the n^{th} gust doublet on the x-axis.

ρ = air density.
 τ = time in units of length, = Ut .
 ϕ, ϕ, ψ = velocity potentials, whose negative gradient yields a corresponding velocity vector.

Subscripts

a = axial flow.
 c = crossflow.
 d = doublet.
 g = gust.
 k = location on x-axis of a steady source or doublet distribution.
 m = time at which a gust doublet starts.
 n = location on x-axis of gust doublet.
 o = upstream (undisturbed) condition.
 r = derivative with respect to r .
 s = source
 st = steady state.
 t = derivative with respect to t .
 x = derivative with respect to x .
 θ = derivative with respect to θ .
 τ = derivative with respect to τ .

Miscellaneous

(prime) = derivative with respect to its independent variable or argument.
 (bar) — = Laplace transform.

ABSTRACT

21720

A theory for predicting [aerodynamic forces on cone-cylinder bodies encountering a step side gust is developed. The theory satisfies the full linearized potential equation, and satisfies the exact boundary condition when steady-state flow has been achieved. This boundary condition is satisfied in an approximate sense in the transient region of flow.

The theory is based on an elementary "gust doublet" solution. In order to arrive at the best fundamental solution for the present purpose, the methods of Laplace transforms, superposition of axial and/or surface singularities, and extensions of older theories are studied. A superposition of basic axial singularities is chosen as the best approach.

The gust doublet solution yields the solution of Tsien when steady-state conditions occur. For this reason, the Karman-Moore technique is relatively simple to apply when complicated body shapes are to be considered.

Author

I. INTRODUCTION

Previous work in the field of unsteady or transient aerodynamic loading of axisymmetric bodies involves many assumptions and simplifications. First, it assumes that the flow field can be described by a potential function. The potential equation is then simplified by neglecting all nonlinear terms, implying that disturbances are small. Furthermore, certain terms in the linearized equation are normally dropped by assuming the body to be slender and/or the reduced frequency to be very large or very small. Also, an approximate boundary condition is normally used, again implying that the body is slender.

The purpose of the present work is to develop a more accurate theory for the indicial aerodynamic forces on a cone-cylinder body encountering a side gust. This theory is based on the full linearized potential equation, but makes use of the exact boundary condition.

II. SUMMARY

A theory for predicting aerodynamic forces on cone-cylinder bodies encountering a step side gust is developed. The theory satisfies the full linearized potential equation, and satisfies the exact boundary condition when steady-state flow has been achieved. This boundary condition is satisfied in an approximate sense in the transient region of flow.

The theory is based on an elementary "gust doublet" solution. In order to arrive at the best fundamental solution for the present purpose, the methods of Laplace transforms, superposition of axial and/or surface singularities, and extensions of older theories are studied. A superposition of basic axial singularities is chosen as the best approach.

The gust doublet solution yields the solution of Tsien when steady-state conditions occur. For this reason, the Karman-Moore technique is relatively simple to apply when complicated body shapes are to be considered.

The linearized lift coefficient for a cone is obtained and compared with that of Miles. The most significant differences are that the gust doublet (1) gives more accurate steady-state results; (2) has no overshoot of the growth of lift curve; and (3) depends on both M and R' , not just the product MR' .

The effect of quadratic terms on the aerodynamic forces is considered. Preliminary results indicate that all such terms must be retained. The nonlinear terms need additional development to facilitate their application. The

gust doublet theory requires additional work to establish more conclusively its accuracy and limits of applicability.

The analysis of accuracy is handicapped by the lack of an exact solution for a cone penetrating a step gust. A numerical technique of obtaining such a solution, making use of the gust doublet, is outlined. This technique has the potential of supplying the desired exact solutions to be used as a basis of comparison.

The gust doublet theory provides the unit step kernel for the Duhamel integral method of calculating responses. The unit impulse kernel, often more convenient, appears to be obtainable from the existing theory by the use of numerical or analytical methods.

III. GENERAL FORMULATION OF THE PROBLEM

The physical problem to be solved can be stated as follows: Find the transient flow field, pressure, etc., on a cone-cylinder body of revolution encountering a side gust while traveling at supersonic speed. Using linearized potential theory, the problem may be stated mathematically as follows:

Find the solution to the linearized potential equation

$$\Phi_{rr} + \frac{1}{r} \Phi_r + \frac{1}{r^2} \Phi_{\theta\theta} - \beta^2 \Phi_{xx} - 2M^2 \Phi_{x\tau} - M^2 \Phi_{\tau\tau} = 0 \quad (3.1)$$

with the boundary conditions

$$\frac{1}{\cos \theta} \Phi_r = -v_o H(\tau-x) \text{ at } r = \infty, \text{ and}$$

$$\Phi_r - R' \Phi_x = 0 \text{ at surface of the body.}$$

We will write the solution as

$$\Phi = \Psi + \phi$$

where

$$\Psi \equiv -v_0 r \cos \theta H(\tau-x) .$$

This has a physical interpretation. The potential, Φ , corresponds to a gust of wind encountering a vehicle with no side displacement. The potential, ϕ , however, gives the impression of a missile suddenly moving sideways into still air. (Of course, there is still axial flow in both cases. We are not concerned with this here.)

Now, Ψ satisfies Eq. (3.1) and likewise, ϕ must satisfy (3.1). The boundary conditions become

$$\phi_r = 0 \quad \text{at} \quad r = \infty \quad (3.2)$$

$$\phi_r - R'\phi_x = v_0 \cos \theta H(\tau-x) \quad \text{at the body, } r = R(x) . \quad (3.3)$$

The right hand side of (3.3) is commonly termed the downwash. Most authors start with the conditions (3.2) and (3.3) or approximations of these. It is important to realize that although Eq. (3.3) indicates a discontinuity in the flow along the body, the complete solution, including Ψ , has no such discontinuity at the body.

An additional comment will be made at this point. The velocity potential is defined here as the negative of the gradient of the velocity vector. All authors are not in agreement as to whether the positive or negative sign will be used. As long as it is clear which is used in a given article, however, no confusion need arise.

IV. A BRIEF REVIEW OF THE LITERATURE

This section reviews those works which most affected the present report; it is not an exhaustive survey, however. Many of the papers mentioned here contain excellent reviews of other related studies.

This report is concerned with the indicial aerodynamic theory for bodies of revolution. An excellent discussion concerning indicial aerodynamics for wings has been written by Lomax [28]. Although the basic approaches set forth these are applicable to the body of revolution, the details are quite different and, in general, more complex in the present case.

* Numbers in brackets refer to the bibliography.

It should be realized that the considerable amount of work on non-linear theory is not mentioned here. The assumptions of linearized potential flow, nonexistence of shock waves, etc., imply that the similarity parameter, $\beta\delta$, is small (less than one in any case). The Saturn V has a nose angle of 33 degrees, requiring that the Mach number be less than about 1.8 for successful application of potential theory. Also, a detached shock wave is produced by this cone when $M < 1.6$, in which case this work would not be accurate, at least near the nose.

The work on steady flow over axially symmetric bodies will be discussed first, since many of the techniques developed there are extendable to the nonsteady problems. The work of Theodor von Karman and Norton B. Moore [1], known in short as the Karman-Moore theory, serves as a good place to start. They considered axial, steady flow over a pointed body, and obtained a source-type solution. They then developed a numerical technique of summing, or superposing such solutions to match arbitrary body shapes. The crossflow problem was studied later in the same manner by Tsien [2]. This is discussed in detail in Appendix A.

The above formulations can be looked upon as first approximations of analytic solutions for arbitrary slender bodies [3], rather than as numerical techniques. This approach was extended to higher order terms by Lighthill [4], Ward [5] and Broderick [6]. A serious question concerning the validity of this technique when the body has a discontinuous slope was raised by Lighthill [7]. He then developed a scheme to handle this type of situation, by means of Stieltjes integrals. Adams and Sears [8] use an expansion technique on the Laplace or Fourier transformed solution which is applicable to not so slender bodies. Finally, Ta Li [9] considers the coupling effect between axial and crossflow.

In the field of nonsteady problems, the case of oscillatory motions offers the greatest abundance of work. Platzler [10] presents a generalization of the Karman-Moore technique which is applied to slowly oscillating bodies. Dorrance [11] developed an analytic solution which serves as an approximation for slender bodies and low-frequency oscillations. This was extended to higher order terms in the reduced frequency by Lansing [12], and a somewhat more general approach was taken by Bond and Packard [13] (see Appendix C). This was still limited to slender bodies, however. Zartarian and Ashley [14] extended the Adams-Sears technique to include the oscillatory case, and Platzler [15] showed that their results can be obtained by means of the Dorrance approach. Also, there is the work of a similar nature by Dzygadlo [16] who considers a body whose surface undergoes small vibrations of a rather general nature.

Not so much work has been done, however, with the indicial case. Miles [17] considers the transient motion of a body of revolution, assuming the body to be very slender and using a high-frequency approximation. This idea was applied to cone-cylinder bodies by Yates [18,19] and Blackburn [20]. These

latter studies all were concerned with both unit step and unit impulse responses. Also, Strang [21] investigated some basic transient solutions of the linearized potential equation. See Section VI for a discussion of this.

In order to develop a more accurate aerodynamic theory for the response to gust loading, there seems to be basically two approaches open. One is the Adams-Sears not so slender body theory; the other being a generalization of the Karman-Moore technique.

The slender body theory of Miles could conceivably be used as a starting point for an Adams-Sears iteration. The prime objection here is the discontinuous body slope which occurs in the Saturn V, and indeed, in most present day missiles. The only satisfactory way to handle this would seem to be along the lines of Lighthill.

The Adams-Sears method might also be applied to the solution of Bond and Packard, although the same arguments again apply. Here it is not clear how to relax the author's approximation for the Bessel function which is made.

An extension of the Karman-Moore theory was chosen as being the better approach. A basic solution with which to work was investigated first by means of the Laplace transform (Section V), and then by a more direct physical approach (Sections VI and VII). An approximation of the solution was found by means of a modification of the paper of Bond and Packard (Appendix C). A brief study of the possibility of assembling nonaxial sources was also made (Appendix B).

V. DERIVATION OF A CLASS OF SOLUTIONS OF EQUATION (3.1)

It appears that an exact solution of (3.1) which satisfies (3.2) and (3.3) will not be found. Various authors have found approximate solutions by making slender body assumptions of various types, or, assuming very high-frequency response, so that axial derivatives in (3.1) may be neglected as compared to time derivatives.

In the present work, we will attempt to use the Karman-Moore technique of superposing solutions of (3.1) in such a way as to satisfy (3.3) at a finite number of points on the body surface. In this section, classes of exact solutions of Eq. (3.1) will be found. They demonstrate the type of behavior to be expected of this equation and give mathematical and physical insight into the problem.

Let

$$\psi(r,p,s) = \int_0^\infty e^{-px} \int_0^\infty e^{-s\tau} \phi(r,x,\tau) dx d\tau .$$

That is, we take Laplace transforms on x and τ . In addition, we have assumed a cosine dependence on θ which is not written, for brevity. Then, Eq. (3.1) becomes

$$\psi_{rr} + \frac{1}{r} \psi_r - \left(\frac{1}{r^2} + \beta^2 p^2 + 2M^2 ps + M^2 s^2 \right) \psi = 0 . \quad (5.1)$$

A general solution of (5.1) is

$$\psi(r,p,s) = F(p,s) K_1 \left(r \sqrt{\beta^2 p^2 + 2M^2 ps + M^2 s^2} \right) , \quad (5.2)$$

K_1 being the modified Bessel function of the second kind, and F an arbitrary function of p and s .

In order to make the required inversions, assume that one can write

$$F(p,s) = \frac{A f(s)}{\sqrt{\beta^2 p^2 + 2M^2 ps + M^2 s^2}} \quad (5.3)$$

where A is a constant. The x -inversion can be performed by letting

$$p = \frac{M}{\beta^2} (\xi - Ms) .$$

Thus,

$$\bar{\phi}(x, r, s) = \frac{Af(s)e^{-\frac{M^2sx}{\beta^2}}}{2\pi i\beta} \int_{c-i\infty}^{c+i\infty} \frac{e^{\frac{Mx\xi}{\beta^2}} K_1\left(\frac{rM}{\beta} \sqrt{\xi^2 - s^2}\right)}{\sqrt{\xi^2 - s^2}} d\xi \quad (5.4)$$

Now, the inverse can be found as [22]

$$\bar{\phi}(x, r, s) = \frac{Af(s)e^{-\frac{M^2sx}{\beta^2}}}{Mrs} \sinh \left[\frac{Ms}{\beta^2} \sqrt{x^2 - \beta^2 r^2} \right] \quad (5.5)$$

where we have used [23] or [24]

$$I_{1/2}(Z) = \sqrt{\frac{2}{\pi Z}} \sinh(Z) \quad .$$

Now, $f(s)$ is an arbitrary function of s . Normally the boundary conditions are used to determine such functions. However, our interest at present is only to find a class of solutions of (3.1) which may be used by means of superposition in the Karman-Moore sense. Since an inversion in time is still required, we will choose $f(s)$ in such a way that the inversion is defined, and may be carried out. This can be done by choosing

$$f(s) = \frac{1}{s^n}, \quad n \geq 0 \quad .$$

Now,

$$L^{-1}\left(\frac{e^{-ks}}{s^m}\right) = \begin{cases} 0, & \tau < k \\ \frac{(\tau-k)^{m-1}}{\Gamma(m)}, & \tau \geq k \end{cases} \quad (5.6)$$

By writing the sinh in (5.5) in terms of exponentials, we have

$$\bar{\phi} = \frac{A}{2Mr} \frac{1}{s^{n+1}} \left\{ e^{-\frac{M}{\beta^2} (Mx - \sqrt{x^2 - \beta^2 r^2})s} - e^{-\frac{M}{\beta^2} (Mx + \sqrt{x^2 - \beta^2 r^2})s} \right\} \quad (5.7)$$

The following facts are noted at this point. To obtain a real (physical) solution, we require that

$$x^2 > \beta^2 r^2 \quad .$$

That is, the body must lie within the Mach cone attached to the nose of the body. Furthermore, it is obvious that in supersonic flow,

$$Mx \geq \sqrt{x^2 - \beta^2 r^2} \quad .$$

Hence, both exponents are negative and the inverse exists. Taking the inverse of (5.7) using (5.6) yields

$$\phi(x, r, \tau) = \frac{A}{2Mr} \left\{ \frac{\left[\tau - \frac{M}{\beta^2} (Mx - \sqrt{x^2 - \beta^2 r^2}) \right]^n}{\Gamma(n+1)} H \left[\tau - \frac{M}{\beta^2} (Mx - \sqrt{x^2 - \beta^2 r^2}) \right] - \frac{\left[\tau - \frac{M}{\beta^2} (Mx + \sqrt{x^2 - \beta^2 r^2}) \right]^n}{\Gamma(n+1)} H \left[\tau - \frac{M}{\beta^2} (Mx + \sqrt{x^2 - \beta^2 r^2}) \right] \right\} \quad (5.8)$$

where H is the unit step function.

Equation (5.8) then represents a class of solutions of (3.1). Before discussing these solutions, it may be mentioned that any sum of such solutions is also a solution. In fact, it may be shown by direct substitution that a more general solution is

$$\phi(x, r, \tau) = \frac{A}{r} \left\{ g \left[\tau - \frac{M}{\beta^2} (Mx - \sqrt{x^2 - \beta^2 r^2}) \right] H \left[\tau - \frac{M}{\beta^2} (Mx - \sqrt{x^2 - \beta^2 r^2}) \right] \right. \\ \left. - g \left[\tau - \frac{M}{\beta^2} (Mx + \sqrt{x^2 - \beta^2 r^2}) \right] H \left[\tau - \frac{M}{\beta^2} (Mx + \sqrt{x^2 - \beta^2 r^2}) \right] \right\} \quad (5.9)$$

where $g(Z)$ is an arbitrary function of Z .

The solutions presented in (5.8) and (5.9) are in some sense discontinuous. That is, the form of the solution is different in different regions of space. First of all, of course, it is required that $x > \beta r$. The locus of points where the arguments of the step functions vanish determine the limits of other regions. Figure 1 shows these regions in the x - r plane.*

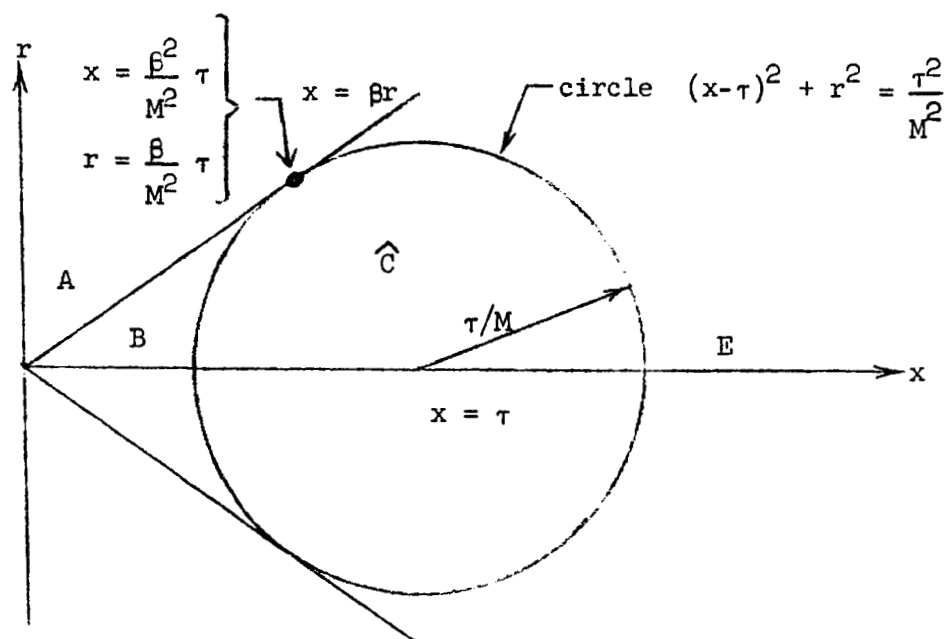


Fig. 1 - Regions of Influence Determined by Eq. (5.8) or (5.9)

* Although the problem is three-dimensional, it is easier to speak in terms of geometry in a plane. The line and circle shown are, in reality, a cone and a sphere. We shall continue to speak in terms of the x - r plane from time to time for simplicity.

The four regions, A, B, \hat{C} , and E each require a different form of ϕ . For example, using Eq. (5.8) with $n = 1$ gives

$$\begin{aligned}
 &\text{For Region E: } \tau < \frac{M}{\beta^2} (Mx - \sqrt{x^2 - \beta^2 r^2}) \\
 &\quad \phi = 0 \quad . \\
 &\text{For Region } \hat{C}: \frac{M}{\beta^2} (Mx - \sqrt{x^2 - \beta^2 r^2}) < \tau < \frac{M}{\beta^2} (Mx + \sqrt{x^2 - \beta^2 r^2}) \\
 &\quad \phi = \frac{A}{2Mr} \left[\tau - \frac{M}{\beta^2} (Mx - \sqrt{x^2 - \beta^2 r^2}) \right] . \\
 &\text{For Region B: } \tau > \frac{M}{\beta^2} (Mx + \sqrt{x^2 - \beta^2 r^2}) \\
 &\quad \phi = \frac{A}{\beta^2 r} \sqrt{x^2 - \beta^2 r^2} \quad . \\
 &\text{For Region A: } x < \beta r \\
 &\quad \phi = 0 \quad .
 \end{aligned} \tag{5.10}$$

Thus, for this case, the potential is zero in Region E, is time-dependent or transient in Region \hat{C} , and is steady in Region B.

The regions in Fig. 1 also have a direct physical interpretation. Using the real time, t , the equation of the circle (actually, a sphere) is

$$(x - Ut)^2 + r^2 = a^2 t^2 \quad .$$

That is, the center is at the leading edge of the gust front, and the radius of the sphere corresponds to the distance traveled in time t by a disturbance propagating at the speed of sound.

The solutions given in (5.8) and (5.9) do not have the r -dependence which is normally seen in the literature. Another set of solutions can be easily derived starting with an axial flow problem. In this case, there is no θ -dependence, and Eq. (5.1) takes the form

$$\psi_{rr} + \frac{1}{r} \psi_r - (\beta^2 p^2 + 2M^2 ps + M^2 s^2) \psi = 0 \quad . \quad (5.11)$$

A general solution of this is

$$\psi(r, p, s) = F(p, s) K_0 \left(r \sqrt{\beta^2 p^2 + 2M^2 ps + M^2 s^2} \right) \quad . \quad (5.12)$$

Then, setting

$$p = \frac{M}{\beta^2} (\xi - Ms)$$

and assuming that F is independent of p ; i.e.,

$$F = Af(s) \quad , \quad (5.13)$$

one can invert (5.12) with respect to p to obtain

$$\bar{\phi}(x, r, s) = \frac{Af(s)e^{-\frac{M^2 sx}{\beta^2}}}{\sqrt{x^2 - \beta^2 r^2}} \cosh \left(\frac{Ms}{\beta^2} \sqrt{x^2 - \beta^2 r^2} \right) \quad . \quad (5.14)$$

Again, a form of $f(s)$ is selected that will enable a final inversion, namely

$$f(s) = \frac{1}{s^n} \quad .$$

We then obtain a class of solutions to the axial flow problems.

$$\phi_a = \frac{A}{2 \sqrt{x^2 - \beta^2 r^2}} \left\{ \frac{\left[\tau - \frac{M}{\beta^2} (Mx - \sqrt{x^2 - \beta^2 r^2}) \right]^{n-1}}{\Gamma(n)} H \left[\tau - \frac{M}{\beta^2} (Mx - \sqrt{x^2 - \beta^2 r^2}) \right] + \right. \\ \left. + \frac{\left[\tau - \frac{M}{\beta^2} (Mx + \sqrt{x^2 - \beta^2 r^2}) \right]^{n-1}}{\Gamma(n)} H \left[\tau - \frac{M}{\beta^2} (Mx + \sqrt{x^2 - \beta^2 r^2}) \right] \right\} \quad (5.15)$$

It is well known that a solution to the crossflow problem can be obtained from an axial solution by applying the operator $\cos \theta \frac{\partial}{\partial r}$. If, for convenience, we denote

$$Z^\pm = \tau - \frac{M}{\beta^2} (Mx \pm \sqrt{x^2 - \beta^2 r^2})$$

and consider a more general form of (5.15), namely,

$$\phi_a = \frac{A}{\sqrt{x^2 - \beta^2 r^2}} g(Z^\pm) \quad , \quad (5.16)$$

then we obtain

$$\phi_c = \frac{Ar \cos \theta}{[x^2 - \beta^2 r^2]^{3/2}} \left[\beta^2 g(Z^\pm) \pm M \sqrt{x^2 - \beta^2 r^2} g'(Z^\pm) \right] \quad . \quad (5.17)$$

It is noted that the same regions of influence occur in the solution (5.15) as were shown earlier. It should also be pointed out that the well known elementary steady potentials [25] can be obtained as special cases of (5.16) and (5.17). One merely sets

$$g(Z^\pm) = \text{constant}$$

and obtains

$$\left. \begin{aligned} \phi_a &= \frac{A}{\sqrt{x^2 - \beta^2 r^2}} \\ \phi_c &= \frac{A\beta^2 r \cos \theta}{[x^2 - \beta^2 r^2]^{3/2}} \end{aligned} \right\} \quad (5.18)$$

It appears that a wealth of solutions to Eq. (3.1) can be readily obtained. The problem, of course, is to satisfy the boundary condition. Anticipating a solution embodying the Karman-Moore approach, it is then a matter of choosing that basic or elementary solution which is most convenient to work with. It was found that a clue to this choice was available in the work which follows in Section VI.

VI. TRANSIENT SOURCE AND DOUBLET SOLUTIONS

The paper by W. J. Strang [21] has a direct bearing on the present problem. Some of his work will be reviewed here, together with extensions made in an attempt to solve the gust problem.

Consider an elementary source of strength V which is located at the origin of a fixed coordinate system. If this source emits a pulse at $t = 0$, then the potential at a point a distance $r_s = \sqrt{r^2 + x^2}$ from the origin may be written as

$$\phi = \frac{Va}{4\pi r_s} \delta(at - r_s)$$

where δ is the Dirac delta function. This says, in effect, that the potential is attenuated as $1/r_s$ and that it propagates with the speed of sound. Now, if the source were placed at the point $x = Ut$, $r = 0$ rather than at the origin, then

$$\phi = \frac{Va}{4\pi\rho} \delta(at-\rho) \quad (6.1)$$

where

$$\rho = \sqrt{r^2 + (x-Ut)^2} \quad .$$

Next, consider a point source moving with supersonic speed U . It starts at time $t = 0$ at the position $x = Ut$, reaching the origin of the coordinate system at time t . Alternatively, it can be viewed as a source which is fixed at the origin in a moving coordinate system. In any case, it is assumed that the source emits at a constant rate. The potential can be found by superposition of pulses of the form of (6.1), or, in the limit, by the integral

$$\phi = \frac{Va}{4\pi} \int_0^t \frac{\delta[at-\rho(t)]}{\rho(t)} dt \quad . \quad (6.2)$$

To evaluate this integral, use must be made of the relation

$$\int_{-\infty}^{\infty} g(x) \delta(f(x)) dx = \sum_{i=1}^n g(x_i) \left| \frac{1}{f'(x_i)} \right| \quad (6.3)$$

where the x_i are the roots of $f(x) = 0$. This relation may be easily proved, but is stated here without proof. Now, the roots of

$$at - \sqrt{r^2 + (x-Ut)^2} = 0$$

are simply

$$t_{1,2} = \frac{1}{a\beta^2} \left[Mx \pm \sqrt{x^2 - \beta^2 r^2} \right], \quad t_1 \geq t_2 \quad . \quad (6.4)$$

Thus, there are four cases to consider:

$$\begin{array}{ll}
A: & x < \beta r \\
B: & t > t_1 \\
\hat{C}: & t_2 < t < t_1 \\
E: & t < t_2
\end{array}
\quad \left. \vphantom{\begin{array}{l} A \\ B \\ \hat{C} \\ E \end{array}} \right\} \quad (6.5)$$

where, in the last three cases, we also require $x > \beta r$. These four cases correspond to the Regions A, B, \hat{C} , and E shown in Fig. 1.

Now, consider

$$\begin{aligned}
F &= \frac{1}{\rho(t) \left| \frac{d}{dt} (at - \rho(t)) \right|} \Big|_{t = t_1} \\
F &= \frac{1}{\rho(t) \left| a + \frac{U(x - Ut)}{\rho(t)} \right|} \Big|_{t = t_1} \\
F &= \frac{1}{|a\rho(t) + U(x - Ut)|} \Big|_{t = t_1} .
\end{aligned} \quad (6.6)$$

But, at $t = t_1$, $\rho(t_1) = at_1$. Furthermore, $t_1 \geq 0$. Thus, (6.6) becomes

$$F = \frac{1}{a \left| Mx - a\beta^2 t_1 \right|}$$

and, using (6.4), we get simply

$$F = \frac{1}{a \sqrt{x^2 - \beta^2 r^2}} . \quad (6.7)$$

Combining (6.2), (6.3), (6.5), and (6.7) the potential function may be written as follows:

$$\left. \begin{aligned}
 \text{In Region B: } \phi &= \frac{V}{2\pi \sqrt{x^2 - \beta^2 r^2}} \\
 \text{In Region } \hat{C}: \phi &= \frac{V}{4\pi \sqrt{x^2 - \beta^2 r^2}} \\
 \text{In Regions A and E: } \phi &= 0
 \end{aligned} \right\} \quad (6.8)$$

Equation (6.8) gives the potential due to a point source located at the origin of a coordinate system which is moving with supersonic speed. It started emitting at time $t = 0$.

Consider next a point source at $x = \xi$ in this moving coordinate system, which starts emitting at time $t = \xi/U$. That is, it starts emitting at a later instant, corresponding to the time required for the coordinate system to move a distance ξ . The various regions of influence of this source are shown in Fig. 2, superposed on the regions of influence of the potential given by (6.8).

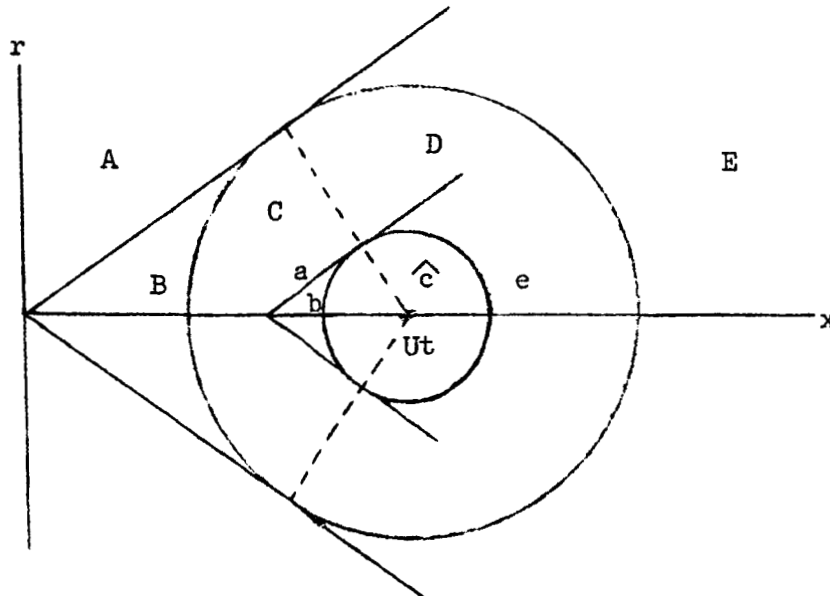


Fig. 2 - Regions of Influence of Moving Point Source

The smaller sphere has the equation

$$(x-Ut)^2 + r^2 = a^2(t-\xi/U)^2 \quad (6.9)$$

while the cone has the equation

$$x = \xi + \beta r \quad .$$

The dotted lines represent the locus of intersections of the spheres and associated cones, and have the equation

$$x = Ut - r/\beta \quad .$$

These lines divide Region \hat{C} into two Regions, C and D.

The point source has the potential ϕ_1 given by

$$\left. \begin{aligned} \phi_{1b} &= \frac{V}{2\pi \sqrt{(x-\xi)^2 - \beta^2 r^2}} \quad \text{in (b)} \\ \phi_{1\hat{C}} &= \frac{V}{4\pi \sqrt{(x-\xi)^2 - \beta^2 r^2}} \quad \text{in } (\hat{C}) \\ \phi_{1e} &= 0 \quad \text{in (e)} \end{aligned} \right\} \quad (6.10)$$

A distribution of sources along the x-axis, where each source starts emitting as it crosses a gust front is called a gust source by Strang. It is this type of distribution that is contemplated here as being a means of finding a solution to the problem of interest. It should be mentioned that ultimately a doublet distribution is desired, but this can be easily obtained from a source distribution.

This gust source will include sources located on the axis between $x = 0$ and $x = Ut$. To obtain the total source potential, ϕ_s , we will have to evaluate the integral

$$\phi_s(x, r, t) = \int_0^\infty \phi_1(x, r; \xi) f(\xi) d\xi \quad (6.11)$$

where ϕ_1 is given in (6.10). The function $f(\xi)$, which may be chosen arbitrarily, represents a possible variation of source strength with position.

The integration of (6.11) is facilitated by Fig. 3.

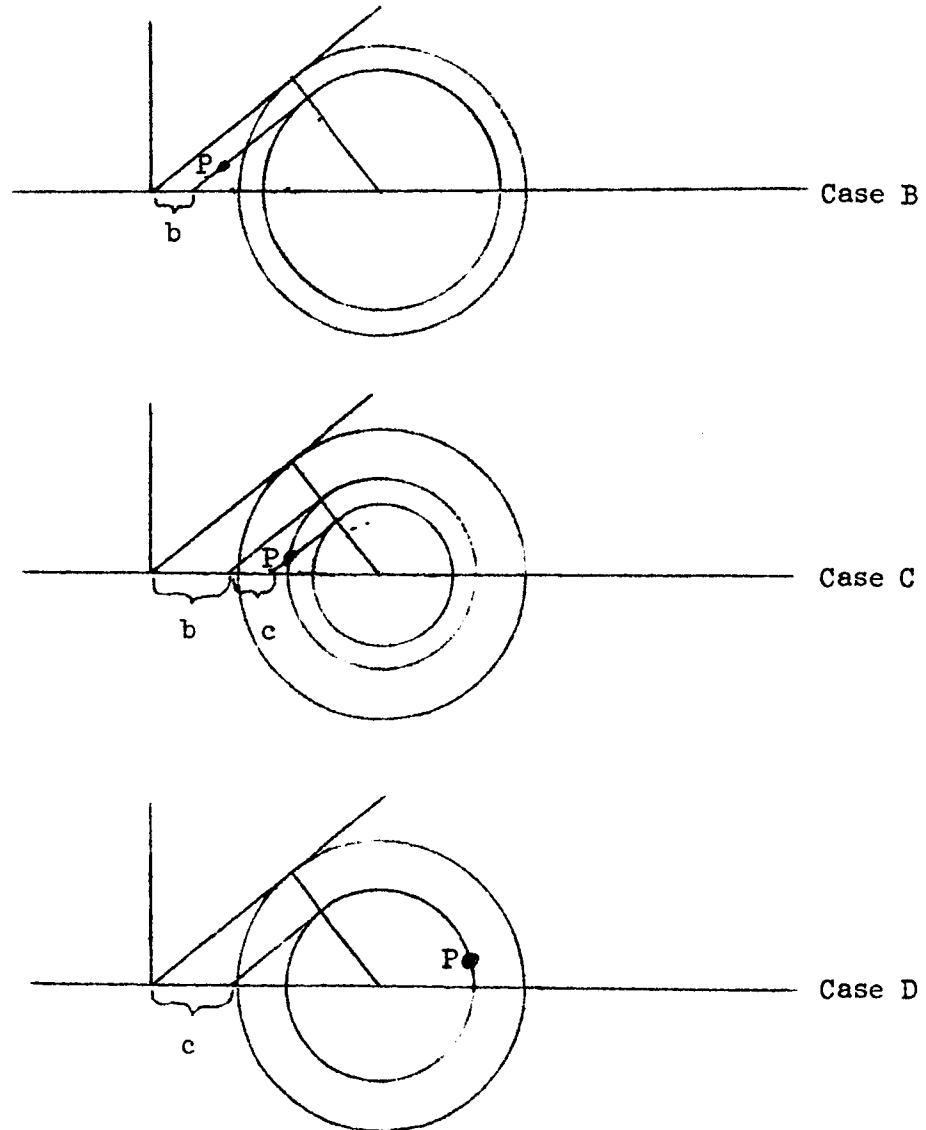


Fig. 3 - Regions of Integration for Eq. (6.11)

There are three nontrivial cases to consider:

Case B: This case corresponds to the situation when the point $P(x, r; t)$ lies in Region B of Fig. 2. In this case, only those sources which are on that portion of the axis labeled as b contribute to the total potential. Furthermore, the point P lies in the corresponding Region b for each of these sources. Thus,

$$\phi_s = \int_0^{x-\beta r} \phi_{1b}(x, r; \xi) f(\xi) d\xi \quad . \quad (6.12)$$

Case C: Here point P lies in Region \hat{C} and is to the left of the line $x = Ut - r/\beta$. Applying the same sort of reasoning as for Case B, yields

$$\phi_s = \int_0^{Ut-M\sqrt{(x-Ut)^2+r^2}} \phi_{1\hat{C}} f(\xi) d\xi + \int_{Ut-M\sqrt{(x-Ut)^2+r^2}}^{x-\beta r} \phi_{1b} f(\xi) d\xi \quad . \quad (6.13)$$

Case D: Now the point P lies in Region \hat{C} but is to the right of the line $x = Ut - r/\beta$. We define this as Region D. Here

$$\phi_s = \int_0^{Ut-M\sqrt{(x-Ut)^2+r^2}} \phi_{1\hat{C}} f(\xi) d\xi \quad . \quad (6.14)$$

Of course, it is easily seen that ϕ_s is zero outside of these regions. The gust source considered by Strang's corresponds to setting $f(\xi) = 1$ (that is, a constant). Carrying out the integrations yields

$$\left. \begin{aligned}
\phi_s &= \frac{V}{2\pi} \cosh^{-1} \left(\frac{x}{\beta r} \right) \quad \text{for Case B} \\
\phi_s &= \frac{V}{4\pi} \left\{ \cosh^{-1} \left(\frac{x}{\beta r} \right) + \cosh^{-1} \left[\frac{x-Ut+M \sqrt{(x-Ut)^2+r^2}}{\beta r} \right] \right\} \quad \text{for Case C} \\
\phi_s &= \frac{V}{4\pi} \left\{ \cosh^{-1} \left(\frac{x}{\beta r} \right) - \cosh^{-1} \left[\frac{x-Ut+M \sqrt{(x-Ut)^2+r^2}}{\beta r} \right] \right\} \quad \text{for Case D} \\
\phi_s &= 0 \quad \text{otherwise.}
\end{aligned} \right\} \quad (6.15)$$

By suitable manipulation, the function ϕ_s for Cases C and D can also be written as

$$\left. \begin{aligned}
\phi_s &= \frac{V}{4\pi} \left\{ \cosh^{-1} \left(\frac{Mx - \sqrt{x^2 - \beta^2 r^2}}{\beta^2 r} \right) - \sinh^{-1} \left(\frac{x-Ut}{r} \right) \right\} \quad \text{in } C^* \\
\phi_s &= \frac{V}{4\pi} \left\{ - \cosh^{-1} \left(\frac{Mx - \sqrt{x^2 - \beta^2 r^2}}{\beta^2 r} \right) - \sinh^{-1} \left(\frac{x-Ut}{r} \right) \right\} \quad \text{in } D^*
\end{aligned} \right\} \quad (6.16)$$

where C^* is that portion of Regions C and D for which

$$x > Mr$$

and D^* is the rest of Regions C and D (see Fig. 4).

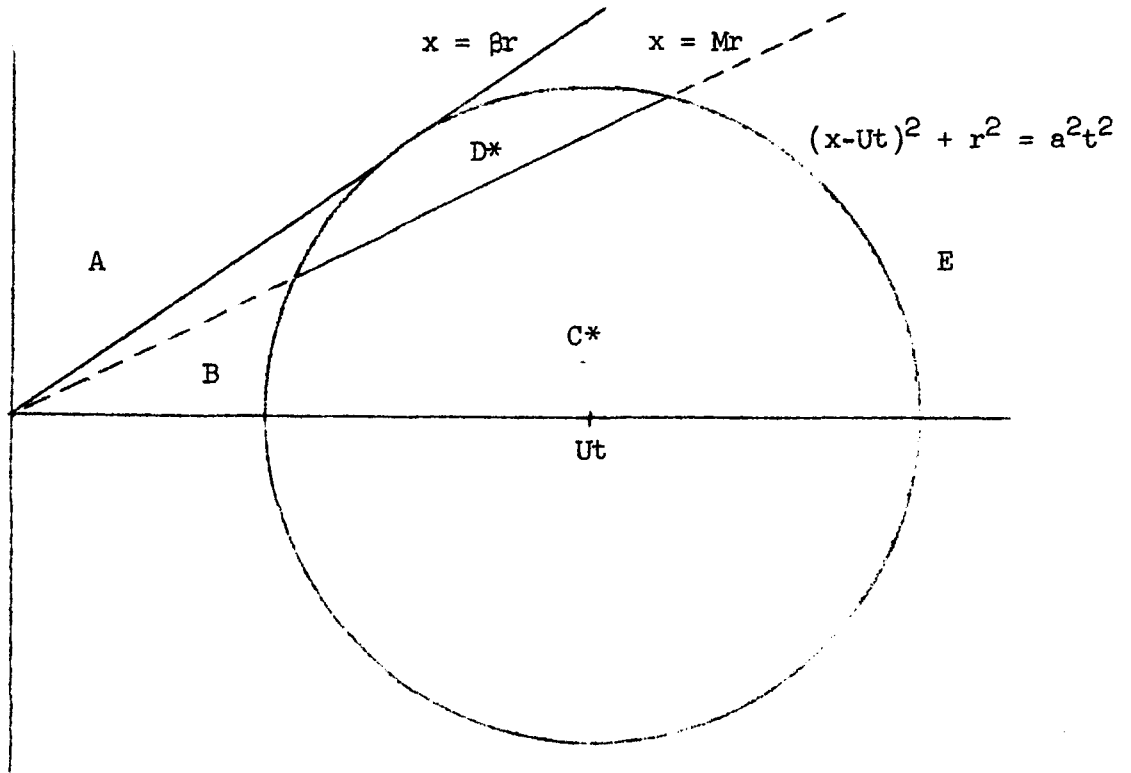


Fig. 4 - Regions of Influence Showing C* and D*

These results agree with those of Strang except for the existence of the relatively small Region D*. His results for the pressures are correct, however. The above expressions for ϕ_s are continuous everywhere, even across the divisions between regions. Certain of the derivatives of ϕ_s are not continuous, but this is no problem, since the derivatives required are continuous.

If one considers a point fixed on the body, with $x > \beta r$, the following sequence of events occurs:

1. Initially there is no disturbance and the potential is zero. The potential remains zero for a time after the source starts emitting, since the point is in Region E.

2. At time $t = \frac{1}{a\beta^2} \left[Mx - \sqrt{x^2 - \beta^2 r^2} \right]$, the potential starts to

change with time. This change continues smoothly, while the spherical region grows and moves downstream. The point may be considered to pass through Region D and then C.

3. At time $t = \frac{1}{a\beta^2} \left[Mx + \sqrt{x^2 - \beta^2 r^2} \right]$ the point has reached Region B and the steady-state value of ϕ has been attained. It will then remain in Region B with a constant potential.

VII. THE GUST DOUBLET SOLUTION FOR A CONE

To use the Karman-Moore technique, it is desirable to first find the solution for flow over a cone. The problem of steady crossflow over a cone was solved by Tsien [2]. We desire a solution of the form of Eq. (6.11) which agrees with Tsien's solution in Region B.

Since this is a doublet solution, we will need to find

$$\phi_d(x, r, t) = \cos \theta \frac{\partial}{\partial r} \int_0^\infty \phi_1(x, r; \xi) f(\xi) d\xi \quad (7.1)$$

It turns out that the required solution is that for which the unknown function, $f(\xi)$, is simply

$$f(\xi) = \xi^2 \quad (7.2)$$

Carrying out the integration of (7.1) using (7.2) and the methods of Section VI, we have

$$\left. \begin{aligned}
\phi_d &= \frac{V \cos \theta}{2\pi} \left\{ \beta^2 r \cosh^{-1} \left(\frac{x}{\beta r} \right) - \frac{x}{r} \sqrt{x^2 - \beta^2 r^2} \right\} \text{ in B} \\
\phi_d &= \frac{V \cos \theta}{4\pi} \left\{ \frac{1}{r \sqrt{(x-Ut)^2 + r^2}} \left[r^2(x+Ut) + x^2(x-Ut) - Mr^2 \sqrt{(x-Ut)^2 + r^2} \right] \right. \\
&\quad \pm \beta^2 r \cosh^{-1} \left[\frac{x-Ut \pm M \sqrt{(x-Ut)^2 + r^2}}{\beta r} \right] \\
&\quad \left. + \beta^2 r \cosh^{-1} \left(\frac{x}{\beta r} \right) - \frac{x}{r} \sqrt{x^2 - \beta^2 r^2} \right\} \text{ in C and D}
\end{aligned} \right\} (7.3)$$

where the upper sign is to be used in Region C and the lower in D. Taking derivatives of (7.3) yields, for Region B,

$$\left. \begin{aligned}
u &= \frac{V\beta \cos \theta}{\pi} \sqrt{\left(\frac{x}{\beta r}\right)^2 - 1} \\
v &= - \frac{V\beta^2 \cos \theta}{2\pi} \left\{ \cosh^{-1} \left(\frac{x}{\beta r} \right) + \frac{x}{\beta r} \sqrt{\left(\frac{x}{\beta r}\right)^2 - 1} \right\} \\
\frac{\partial \phi}{\partial t} &= 0 \quad ;
\end{aligned} \right\} (7.4)$$

while for Regions C and D ,

$$\begin{aligned}
u = & - \frac{V \cos \theta}{4\pi r} \left\{ \frac{1}{[(x-Ut)^2 + r^2]^{3/2}} \left[2Ut(x-Ut)^3 + r^2(x^2 + r^2) \right] \right. \\
& + \left. \frac{1}{[(x-Ut)^2 + r^2]^{1/2}} \left[2(x-Ut)^2 - \beta^2 r^2 \right] - 2 \sqrt{x^2 - \beta^2 r^2} \right\} \\
v = & - \frac{V \cos \theta}{4\pi} \left\{ \frac{(x-Ut)}{r^2 [(x-Ut)^2 + r^2]^{3/2}} \left[2x^3 Ut - (x^2 + r^2)(x^2 + U^2 t^2) \right] \right. \\
& - M + \frac{\beta^2 (x-Ut)}{\sqrt{(x-Ut)^2 + r^2}} \pm \beta^2 \cosh^{-1} \left[\frac{x-Ut+M \sqrt{(x-Ut)^2 + r^2}}{\beta r} \right] \\
& + \left. \beta^2 \left[\cosh^{-1} \left(\frac{x}{\beta r} \right) + \left(\frac{x}{\beta r} \right) \sqrt{\left(\frac{x}{\beta r} \right)^2 - 1} \right] \right\} \\
\frac{\partial \phi}{\partial t} = & \frac{rUV \cos \theta}{4\pi} \left\{ \frac{r^2 - x^2 + 2x(x-Ut)}{[(x-Ut)^2 + r^2]^{3/2}} + \frac{\beta^2}{\sqrt{(x-Ut)^2 + r^2}} \right\}
\end{aligned} \tag{7.5}$$

In Eqs. (7.4) and (7.5) the relations

$$\begin{aligned}
u = & - \frac{\partial \phi}{\partial x} \\
v = & - \frac{\partial \phi}{\partial r}
\end{aligned} \tag{7.6}$$

have been used.

The pressure coefficient may be written as

$$C_P \equiv \frac{p-p_0}{\frac{1}{2} \rho_0 U^2} \approx \frac{2}{U^2} [\phi_t + U \phi_x] \quad (7.7)$$

where we have neglected the squared terms.* This gives

$$C_P = - \frac{2V\beta \cos \theta}{\pi U} \sqrt{\left(\frac{x}{\beta r}\right)^2 - 1} \quad (7.8)$$

in Region B, while in C and D,

$$C_P = \frac{V \cos \theta}{\pi U} \left\{ \frac{r^4 + (x-Ut)[x r^2 + Ut(x-Ut)^2]}{r[(x-Ut)^2 + r^2]^{3/2}} + \frac{(x-Ut)^2}{r[(x-Ut)^2 + r^2]^{1/2}} - \beta \sqrt{\left(\frac{x}{\beta r}\right)^2 - 1} \right\} . \quad (7.9)$$

The solution given in Eqs. (7.3) to (7.9) agrees exactly with Tsien's solution in Region B, the area of steady-state flow. In addition, the complete solution together with the derivatives given above is continuous everywhere.

Now, the above solution satisfies the boundary condition (3.2) at infinity. To satisfy condition (3.3) at the body, one requires that

$$\phi_r - R' \phi_x = v_0 \cos \theta \quad \text{in Region B} \quad (7.10)$$

$$\phi_r - R' \phi_x = v_0 \cos \theta H(Ut-x) \quad \text{in Regions C and D} . \quad (7.11)$$

* See Appendix E for higher order approximations to the pressure coefficient.

Here we have an impasse. Since the solution has but a single arbitrary constant, V , it is, in general, impossible to satisfy both (7.10) and (7.11). Thus, the present method implies an approximation which will be discussed presently.

Since the solution is continuous, Eq. (7.11) cannot be satisfied, so the value of V will be chosen so as to satisfy Eq. (7.10). That is, we will insist that the correct steady-state solution be obtained. Tsien used the approximate (slender body) condition

$$\phi_r = v_0 \cos \theta$$

rather than the exact boundary condition (3.3). It is no more difficult to use the exact condition, so this will be done. Using (7.10), we obtain

$$\frac{V}{\pi} = \frac{2v_0/\beta^2}{\cosh^{-1}\left(\frac{1}{\gamma}\right) + \frac{2\gamma^2/\beta^2 + 1}{\gamma^2} \sqrt{1-\gamma^2}} \quad (7.12)$$

where

$$\gamma = \beta R'$$

R' = slope of cone surface .

It is assumed, of course, that

$$R' < \frac{1}{\beta}$$

so that the body lies inside of the Mach cone.

The amount of error involved in not satisfying Eq. (7.11) can be shown graphically as in Fig. 5, p. 29. In this figure is shown the quantity

$$\frac{\text{Downwash (Calculated)} - \text{Downwash (Exact)}}{\text{Downwash (Steady-State)}}$$

for different cone angles. The calculated downwash is the left-hand side of (7.11) and the exact downwash is the right-hand side of (7.11). The steady-state value is simply $v_o \cos \theta$. A Mach number of two was used here, and the cone location with reference to the Regions B, C, and D is shown in Fig. 6. Fig. 5 shows that the error decreases as R' becomes smaller.

Indeed, as $R' \rightarrow 0$, it can be shown that Eq. (7.11) is satisfied exactly. In other words, the solution requires a slender body approximation in order to satisfy the boundary condition. For R' very small, (7.12) approaches

$$\frac{V}{\pi} \approx 2v_o R'^2 \quad . \quad (7.13)$$

Substituting (7.13) into (7.5) and retaining only the lowest order terms,

$$\begin{aligned} \lim_{R' \rightarrow 0} (\phi_r - R' \phi_x) &= \frac{v_o R'^2 \cos \theta}{2} \left\{ \frac{x - Ut}{R'^2 [(x - Ut)^2]^{3/2}} [2xUt - (x^2 + U^2 t^2)] \right. \\ &\quad \left. + \frac{1}{R'^2} \right\} + O(R') \end{aligned}$$

or,

$$\begin{aligned} \lim_{R' \rightarrow 0} (\phi_r - R' \phi_x) &= \frac{v_o \cos \theta}{2} \left\{ 1 + \frac{-(x - Ut)^3}{[(x - Ut)^2]^{3/2}} \right\} \\ &= v_o \cos \theta H(Ut - x) \quad . \end{aligned} \quad (7.14)$$

The last step holds since $[(Z)^2]^{3/2} = -(Z)^3$ for Z negative.

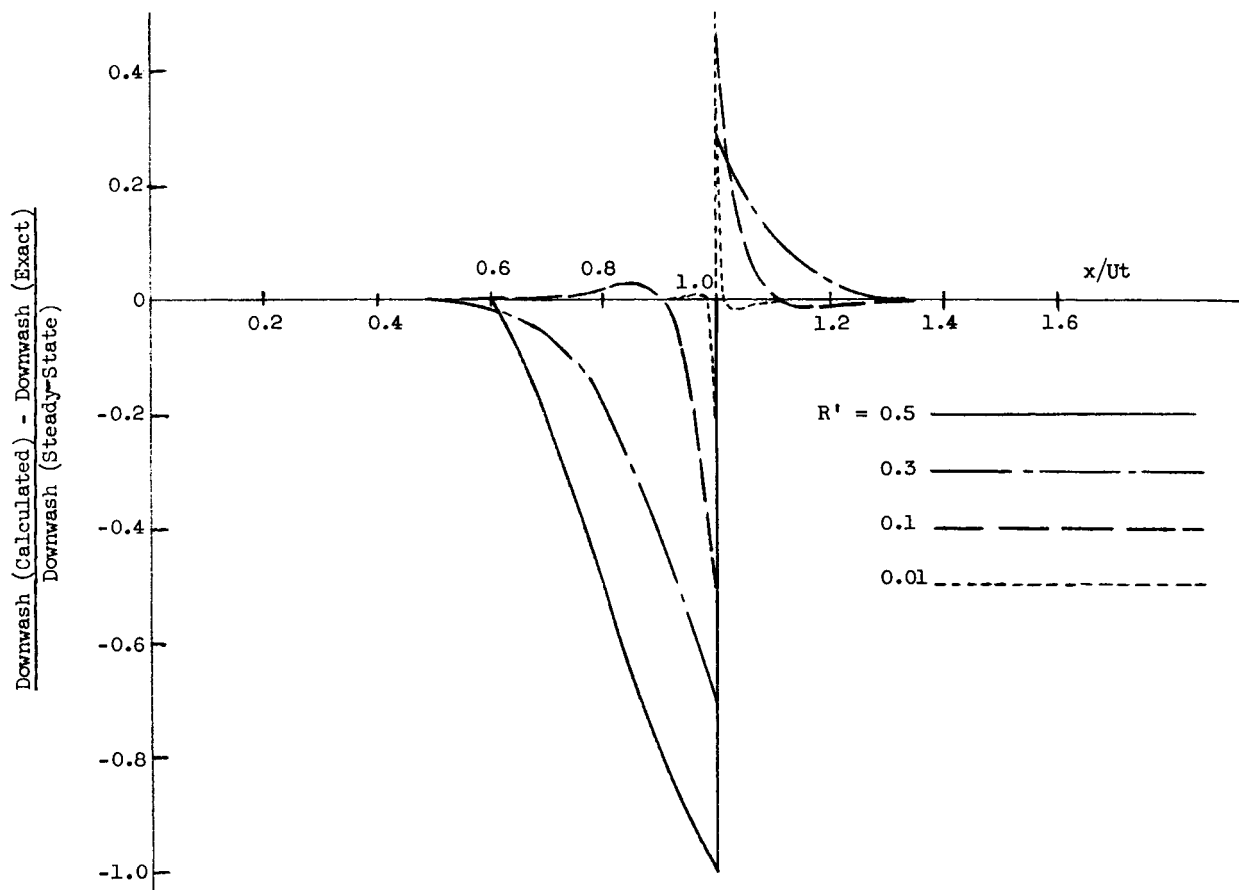


Fig. 5 - Relative Error in Boundary Condition

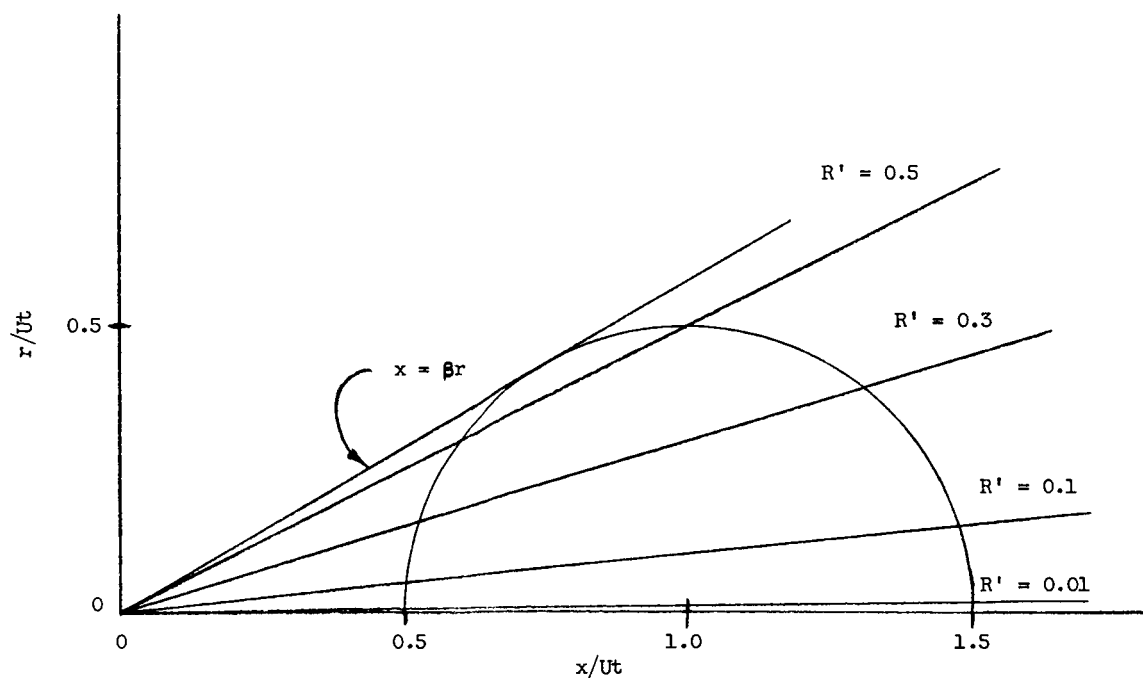


Fig. 6 - Regions of Influence for Various Cones

Heretofore, other authors have found approximate solutions to the potential equation by: (1) neglecting certain terms in the equation by assuming slender body and/or high frequency; and (2) using a slender body approximation for the left-hand side of (7.11). The present theory involves only a slender body approximation for the right-hand side of (7.11).

It cannot be said at this point whether the present solution is any better or worse than previous approximations. However, at least the present solution leads to the correct steady-state values.

The growth of lift will be found next and compared with Miles' [17] results.

The lift coefficient, C_L , is defined as

$$C_L = \frac{1}{S} \int_0^{2\pi} \int_0^1 C_P R' \cos \theta \, x \, dx \, d\theta \quad (7.15)$$

where S is the base area of the cone which is assumed to have unit length. We need to consider three different cases.

1. Part of the cone has not yet been affected by the gust, i.e., part of it lies in Region E.
2. The cone is completely within Regions B, C, and D but not wholly within B.
3. The cone is completely within Region B, i.e., steady state has been reached.

Carrying out the lengthy integrations and simplifying, the results obtained are:

Case 1: $Ut < \frac{1+R'^2}{1 + \frac{1}{M} \sqrt{1-\gamma^2}}$,

$$\frac{C_L}{C_{L_{st}}} = (Ut)^2 \left\{ \frac{(1-R'^2)}{(1+R'^2)^2} + \frac{R'^2 \sinh^{-1} \left(\frac{\sqrt{1-\gamma^2}}{MR'} \right)}{\sqrt{1-\gamma^2} (1+R'^2)^{3/2}} \right\}$$

Case 2: $\frac{1+R'^2}{1 + \frac{1}{M} \sqrt{1-\gamma^2}} < Ut < \frac{1+R'^2}{1 - \frac{1}{M} \sqrt{1-\gamma^2}}$,

$$\frac{C_L}{C_{L_{st}}} = (Ut)^2 \left\{ \frac{1}{2} \frac{\left[1 - \frac{1}{M} \sqrt{1-\gamma^2} \right]^2}{(1+R'^2)^2} + \frac{2 - \frac{\sqrt{1-\gamma^2}}{M}}{2M \sqrt{1-\gamma^2} (1+R'^2)} + \right.$$

$$\left. + \frac{R'^2}{2 \sqrt{1-\gamma^2} (1+R'^2)^{3/2}} \left[\sinh^{-1} \left(\frac{\sqrt{1-\gamma^2}}{MR'} \right) + \sinh^{-1} \left(\frac{1+R'^2-Ut}{R'Ut} \right) \right] \right\}$$

$$- \frac{\sqrt{(1-Ut)^2 + R'^2} (1+R'^2 + Ut)}{2 \sqrt{(1-\gamma^2)} (1+R'^2)} + \frac{1}{2}$$

(7.16)

Case 3: $Ut > \frac{1+R'^2}{1 - \frac{1}{M} \sqrt{1-\gamma^2}}$,

$$\frac{C_L}{C_{L_{st}}} = 1$$

where the steady-state lift coefficient is

$$C_{L_{st}} = \frac{2 \sqrt{1-\gamma^2} (v_0/U)}{\gamma^2 \cosh^{-1}\left(\frac{1}{\gamma}\right) + (1+2R'^2) \sqrt{1-\gamma^2}} \quad (7.17)$$

Figure 7 shows $C_L/C_{L_{st}}$ plotted against Ut for $MR' = 0.3$. The result of Miles is also shown. The most significant differences are as follows:

1. Miles' results depend on the single parameter $\alpha = MR'$, while the present case depends on both M and R' .
2. There is no "overshoot" in the present theory.
3. Steady state is reached in a finite time.
4. The growth of lift is continuous and differentiable, that is, there is no "knee" in the curve.

In addition, the steady-state lift predicted by the present theory is in agreement with the exact steady flow results, whereas Miles' theory predicts the slender body result of $2v_0/U$ (see Fig. 8).

In the future, it would be highly desirable to obtain a numerical solution of Eq. (3.1) satisfying (3.3) for a cone of finite semiapex angle. This would allow a comparison of various theories, as well as possibly providing more insight into the phenomena involved. A possible approach to such a solution is presented in Appendix D.

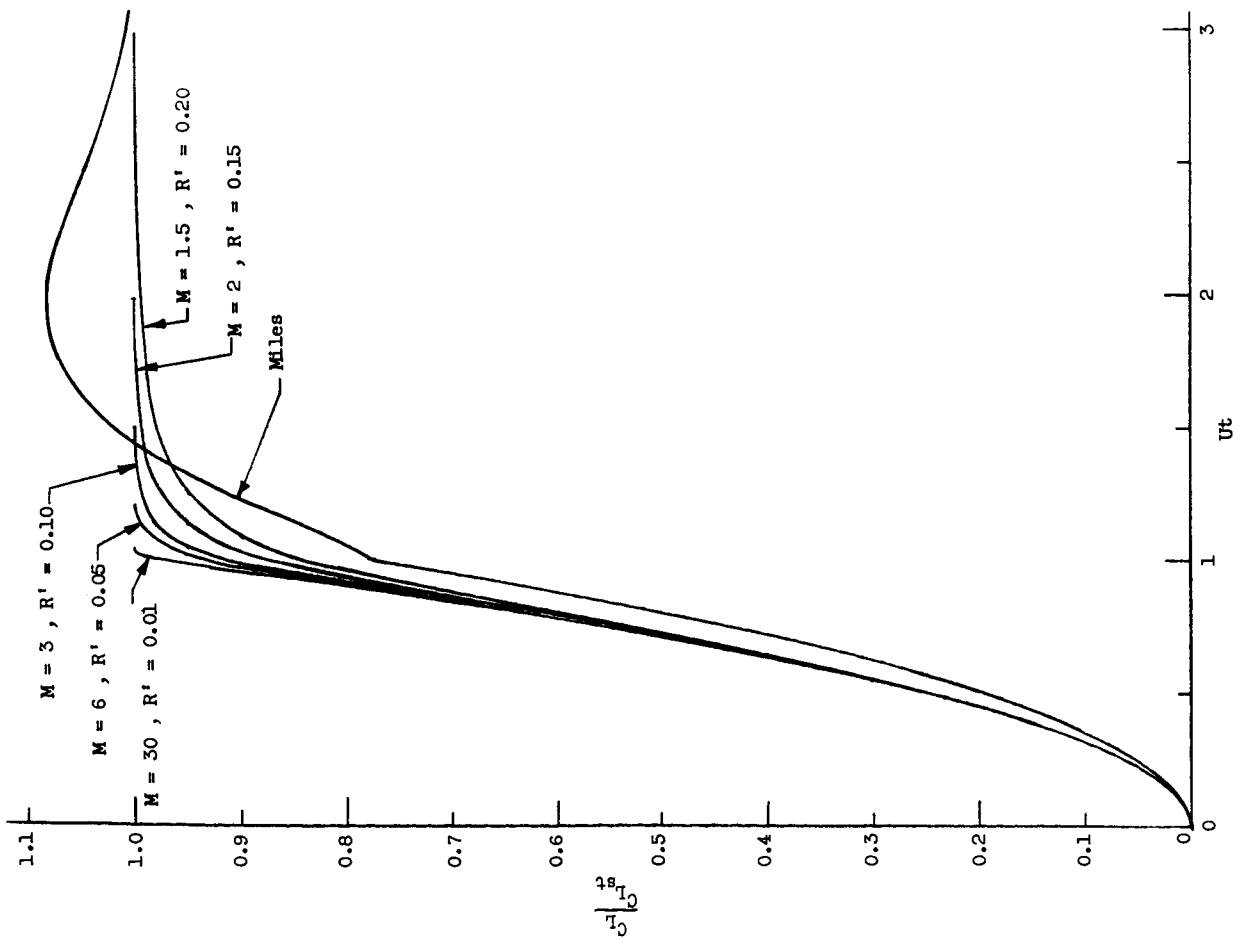


Fig. 7 - Growth of Lift for $MR' = 0.3$

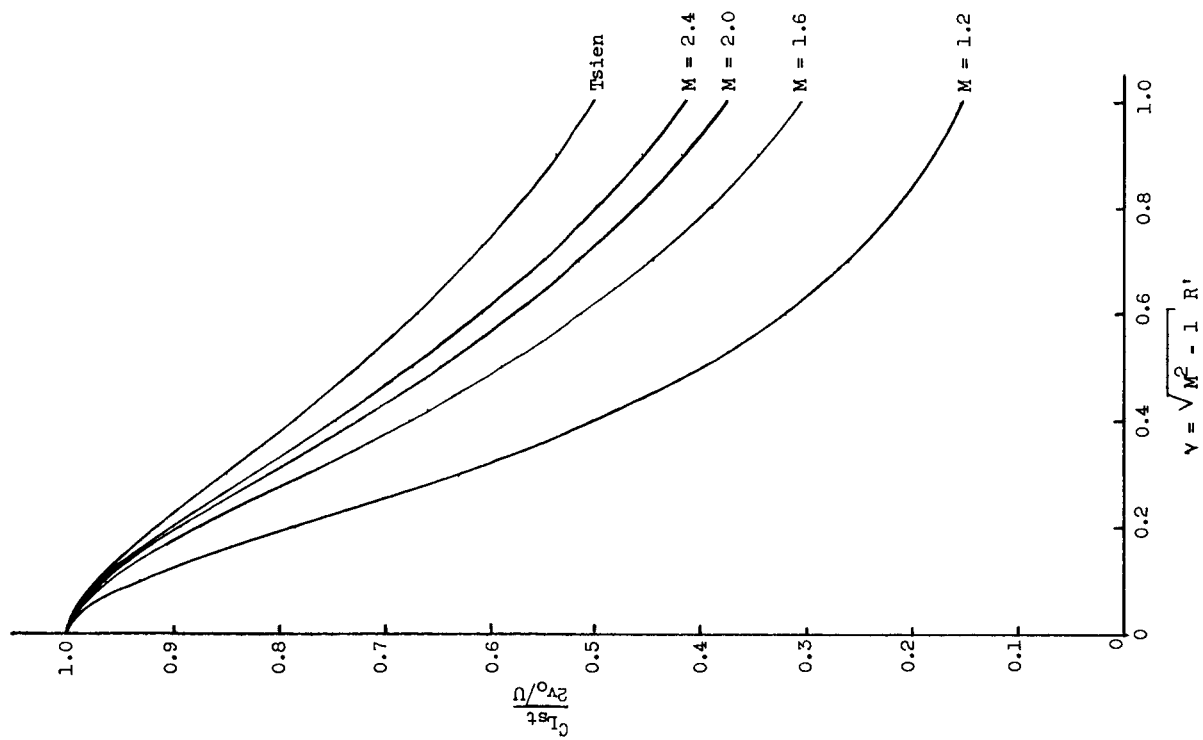


Fig. 8 - Steady-State Lift Coefficients

VIII. GENERALIZED FORCE COEFFICIENTS

This section contains the derivation and tabulation of various coefficients which are required in the next section. These coefficients are the normal force or lift coefficient, the moment coefficient, and a third coefficient called the bending moment coefficient. We call these, collectively, the generalized force coefficients. These will be defined by

$$C_{F_\ell} = \frac{\pi}{SL^\ell} \int C_P x^\ell R \, dx \quad (8.1)$$

where C_{F_ℓ} is the ℓ^{th} generalized force coefficient, S is a reference area (here the base area of the body), L is the reference length (length of body), and $R(x)$ is the profile shape. By setting $\ell = 0, 1$, and 2 we get C_L , C_M , and C_B , respectively. The latter is required in the missile bending equations, when the mode shape is approximated by a quadratic.

Equation (8.1) contains no angular dependence. It has already been integrated out. Therefore, in the remainder of this section no references will be made to the $\cos \theta$ dependence of the potential function and its derivatives.

It is most advantageous to express (8.1) in terms of indefinite integrals, in a rather general form. This is due to the fact that a numerical procedure, which is an extension of the Karman-Moore technique, is contemplated. In addition, the many different forms of limits (of the integrals) which can occur, together with the complexity of the expressions make it most efficient to use indefinite integrals. The limits can then be substituted into the expression numerically by the computer program.

For the purposes of this section, the approximate (linear) expression

$$C_P = \frac{2}{U^2} (\phi_t + U\phi_x) \quad (8.2)$$

will be used. The nonlinear terms are considered in Appendix E.

The profile shape, $R(x)$, will be taken as a frustrum of a cone, with the equation

$$R(x) = R'x + P \quad (8.3)$$

By properly choosing R' and P , any desired segment of a cone-cylinder body can be correctly expressed by (8.3).

Now, since the gust doublet will be used as a basic solution in the Karman-Moore approach, a slightly more general form of this doublet will be needed. It is sufficient to consider a gust doublet which starts at an arbitrary point ξ_n on the x-axis at the time t_m (see Fig. 9).

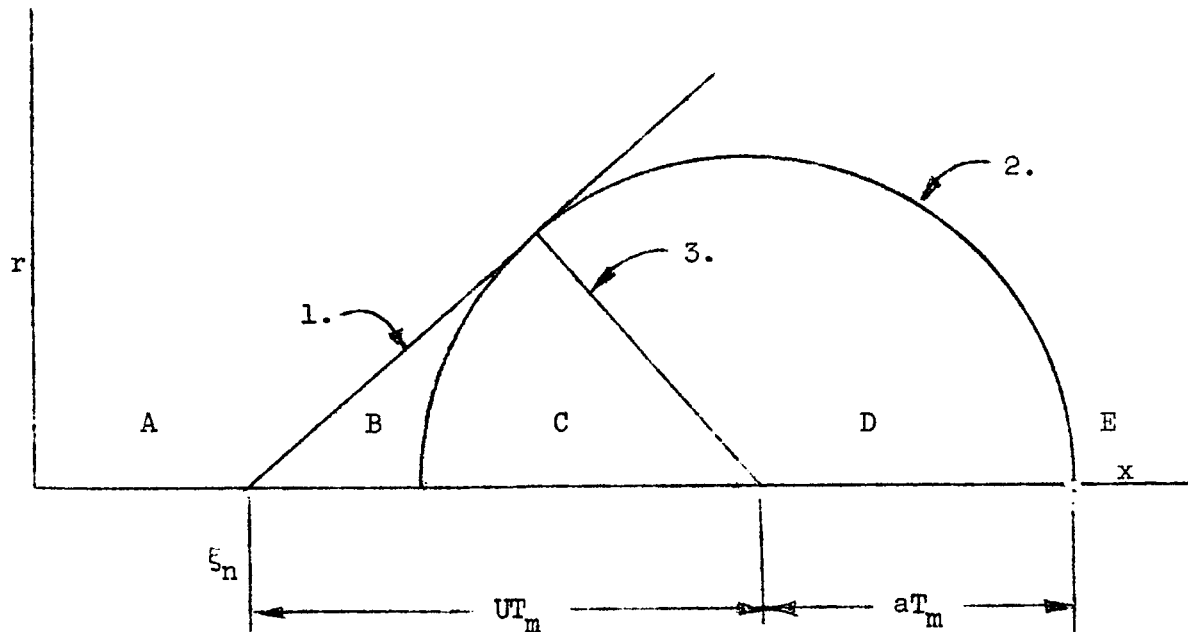


Fig. 9 - General Gust Doublet

In this figure, the equations of the surfaces which define the regions are:

$$1. \quad X_n = \beta r \quad (8.4)$$

$$2. \quad (X_n - UT_m)^2 + r^2 = a^2 T_m^2 \quad (8.5)$$

$$3. \quad X_n = UT_m - r/\beta \quad (8.6)$$

where we have introduced the notation

$$X_n = x - \xi_n \quad (8.7)$$

$$T_m = t - t_m \quad (8.8)$$

We then have, in Region B,

$$\phi = \frac{A_{mn}}{2\pi} \left\{ \beta^2 r \cosh^{-1} \left(\frac{X_n}{\beta r} \right) - \frac{X_n}{\beta r} \sqrt{X_n^2 - \beta^2 r^2} \right\} \quad (8.9)$$

$$\phi_x = - \frac{A_{mn}\beta}{\pi} \sqrt{\left(\frac{X_n}{\beta r} \right)^2 - 1} \quad (8.10)$$

$$\phi_r = + \frac{A_{mn}\beta^2}{2\pi} \left\{ \cosh^{-1} \left(\frac{X_n}{\beta r} \right) + \frac{X_n}{\beta r} \sqrt{\left(\frac{X_n}{\beta r} \right)^2 - 1} \right\} \quad (8.11)$$

$$\frac{\partial \phi}{\partial t} = 0 \quad (8.12)$$

while in Regions C and D (upper signs used in C)

$$\phi = \frac{A_{mn}}{4\pi} \left\{ \pm \beta^2 r \cosh^{-1} \left[\frac{X_n - UT_m + M \sqrt{(X_n - UT_m)^2 + r^2}}{\beta r} \right] + \frac{r^2 (X_n + UT_m) + X_n^2 (X_n - UT_m) - Mr^2 \sqrt{(X_n - UT_m)^2 + r^2}}{r \sqrt{(X_n - UT_m)^2 + r^2}} \right\} \quad (8.13)$$

$$\phi_x = + \frac{A_{mn}}{4\pi r} \left\{ \frac{1}{[(X_n - UT_m)^2 + r^2]^{3/2}} \left[2UT_m (X_n - UT_m)^3 + r^2 (X_n^2 + r^2) \right] + \frac{1}{[(X_n - UT_m)^2 + r^2]^{1/2}} \left[2(X_n - UT_m)^2 - \beta^2 r^2 \right] - 2\beta r \sqrt{\left(\frac{X_n}{\beta r}\right)^2 - 1} \right\} \quad (8.14)$$

$$\phi_r = + \frac{A_{mn}}{4\pi} \left\{ \frac{(X_n - UT_m)}{r^2 [(X_n - UT_m)^2 + r^2]^{3/2}} \left[2X_n^3 UT_m - (X_n^2 + r^2)(X_n^2 + U^2 T_m^2) \right] - M + \frac{\beta^2 (X_n - UT_m)}{[(X_n - UT_m)^2 + r^2]^{1/2}} \pm \beta^2 \cosh^{-1} \left[\frac{X_n - UT_m + M \sqrt{(X_n - UT_m)^2 + r^2}}{\beta r} \right] + \beta^2 \left[\cosh^{-1} \left(\frac{X_n}{\beta r} \right) + \left(\frac{X_n}{\beta r} \right) \sqrt{\left(\frac{X_n}{\beta r}\right)^2 - 1} \right] \right\} \quad (8.15)$$

$$\phi_t = \frac{rUA_{mn}}{4\pi} \left\{ \frac{r^2 - X_n^2 + 2X_n (X_n - UT_m)}{[(X_n - UT_m)^2 + r^2]^{3/2}} + \frac{\beta^2}{\sqrt{(X_n - UT_m)^2 + r^2}} \right\} \quad (8.16)$$

The expressions (8.10), (8.12), (8.14), and (8.16) may then be placed into (8.1), using the relation for C_p given in (8.2). The integrals may then be evaluated on the segment of surface given in (8.3). The resulting force coefficients are given as (8.17) to (8.19) for Region B and (8.20) to (8.22) for C and D.

In B:

$$C_{F_0} = C_L = - \frac{A_{mn}}{SU(1-\gamma^2)} \left\{ \left[(1-\gamma^2)x - (\xi_n + \beta^2 PR') \right] \sqrt{Y} - \frac{\beta^2}{\sqrt{1-\gamma^2}} (P+R'\xi_n)^2 \cosh^{-1} \bar{Y} \right\} \quad (8.17)$$

$$C_{F_1} = C_M = - \frac{2A_{mn}}{SLU(1-\gamma^2)} \left\{ \frac{1}{3} Y^{3/2} \right\} + \frac{\xi_n + \beta^2 PR'}{L(1-\gamma^2)} C_L \quad (8.18)$$

$$C_{F_2} = C_B = - \frac{A_{mn}}{6SL^2U(1-\gamma^2)^2} \left\{ \left[3(1-\gamma^2)x + 5(\xi_n + \beta^2 PR') \right] Y^{3/2} \right\} + \frac{5(\xi_n + \beta^2 PR')^2 - (1-\gamma^2)(\xi_n^2 - \beta^2 P^2)}{4(1-\gamma^2)^2 L^2} C_L \quad (8.19)$$

In C and D:

$$C_{F_0} = C_L = \frac{A_{mn}}{2SU(1+R'^2)} \left\{ \left[(1+R'^2)x + PR' - \xi_n + UT_m \right] Z^{1/2} + \frac{\left[R'(\xi_n + UT_m) + P \right]^2 - 2UT_m \left[PR' + R'^2(\xi_n + UT_m) \right]}{\sqrt{1+R'^2}} \sinh^{-1} \bar{Z} \right\} + \frac{1}{2} C_L \text{ (Region B)} \quad (8.20)$$

$$\begin{aligned}
C_{F_1} = C_M = & \frac{A_{mn}}{SLU(1+R'^2)} \left\{ \frac{1}{3} Z^{3/2} \right. \\
& + UT_m \left[2(1+R'^2)(\xi_n + UT_m)(PR' - \xi_n - UT_m) + 3(PR' - \xi_n - UT_m)^2 \right. \\
& \left. \left. - (1+R'^2)(P^2 + (\xi_n + UT_m)^2) \right] \frac{\sinh^{-1} \bar{Z}}{2(1+R'^2)^{3/2}} \right. \\
& - \frac{[PR' - \xi_n - UT_m][R'(\xi_n + UT_m) + P]^2 \sinh^{-1} \bar{Z}}{2(1+R'^2)^{3/2}} \\
& + \frac{UT_m \left[(1+R'^2)x - 3(PR' - \xi_n - UT_m) - 2(1+R'^2)(\xi_n + UT_m) \right] Z^{1/2}}{2(1+R'^2)} \\
& - \frac{[PR' - \xi_n - UT_m] \left[(1+R'^2)x + PR' - \xi_n - UT_m \right] Z^{1/2}}{2(1+R'^2)} \\
& \left. + \frac{1}{2} C_M (\text{Region B}) \right\} . \tag{8.21}
\end{aligned}$$

$$\begin{aligned}
C_{F_2} = C_B = & \frac{A_{mn}}{2SL^2U(1+R'^2)^2} \left\{ \frac{3(1+R'^2)x-5(PR' - \xi_n - UT_m)}{6} Z^{3/2} \right. \\
& + \frac{\left[5(PR' - \xi_n - UT_m)^2 - (1+R'^2)(P^2 + (\xi_n + UT_m)^2) \right] \left[(1+R'^2)x + PR' - \xi_n - UT_m \right] Z^{1/2}}{4(1+R'^2)} \\
& + \frac{UT_m \left[2(1+R'^2)^2 x^2 - 5(PR' - \xi_n - UT_m) \left((1+R'^2)x - 3(PR' - \xi_n - UT_m) \right) \right] Z^{1/2}}{3(1+R'^2)} \\
& - \frac{UT_m \left[4P^2 + 4(\xi_n + UT_m)^2 + 3(\xi_n + UT_m) \left((1+R'^2)x - 3(PR' - \xi_n - UT_m) \right) \right] Z^{1/2}}{3(1+R'^2)} \\
& + \frac{\left[5(PR' - \xi_n - UT_m)^2 - (1+R'^2)(P^2 + (\xi_n + UT_m)^2) \right] \left[R'(\xi_n + UT_m) + P \right]^2 \sinh^{-1} \bar{Z}}{4(1+R'^2)^{3/2}} \\
& - \frac{UT_m \left[PR' - \xi_n - UT_m \right] \left[15(PR' - \xi_n - UT_m)^2 - 9(1+R'^2)(P^2 + (\xi_n + UT_m)^2) \right] \sinh^{-1} \bar{Z}}{3(1+R'^2)^{3/2}} \\
& - \left. \frac{UT_m (\xi_n + UT_m) \left[3(PR' - \xi_n - UT_m)^2 - (1+R'^2)(P^2 + (\xi_n + UT_m)^2) \right] \sinh^{-1} \bar{Z}}{(1+R'^2)^{1/2}} \right\} \\
& + \frac{1}{2} C_B \text{ (Region B)} \quad . \quad (8.22)
\end{aligned}$$

In these equations we have used the abbreviations

$$Y = X_n^2 - \beta^2 (R'x+P)^2 \quad (8.23)$$

$$\bar{Y} = \frac{X_n - \beta^2 R' (R'x+P)}{\beta (R' \xi_n + P)} \quad (8.24)$$

$$Z = (X_n - UT_m)^2 + (R'x+P)^2 \quad (8.25)$$

$$\bar{Z} = \frac{(X_n - UT_m) + R' (R'x+P)}{R' (\xi_n + UT_m) + P} \quad (8.26)$$

IX. APPLICATION OF THE GUST DOUBLET TO CONE-CYLINDER BODIES

The gust doublet solution which was derived and discussed previously can be used as the fundamental solution in a Karman-Moore procedure for an arbitrary body shape. This section presents the detailed procedure to be used for a cone-cylinder body such as the Saturn V configuration.

The basic solution given as Eqs. (8.9) to (8.16) is in a general enough form to be applied directly to a cone-cylinder combination, provided the points ξ_n , the times t_m , and the coefficients A_{mn} are known. To determine these, use is made of the fact that the steady-state solution agrees with the crossflow solution of Tsien.

It is convenient to make use of Tsien's solution directly. That is, first one can choose as "control points" on the body surface the same set as would be used in a steady-flow computation.* The Mach lines through these points intersect the x-axis at the points ξ_n . Now the coefficients A_{mn} can be determined in the standard fashion if the steady-state results (Region B) are used.

To account for the motion of the missile through the gust front, it is logical and consistent to delay the start of emission of the doublets until the gust reaches the local origin, ξ_n . This gives the time, t_m , as**

$$t_m = \xi_n / U \quad (9.1)$$

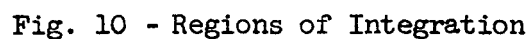
The complete solution is then easily obtained by summing all of the doublet solutions used. The only remaining step is to integrate the summation over the body surface to obtain the desired generalized force coefficients. The expressions (8.17) to (8.22) developed previously can be used for this purpose, in the manner next described.

* See Appendix A for a discussion of the procedure.

** The subscripting notation now becomes somewhat superfluous since m and n are no longer independent. To avoid future complications, however, it is best to retain both subscripts and make use of (9.1) when applicable.

Consider a straight line segment, representing a portion of the missile surface, given by the equation

This segment extends from $x = x_a$ to $x = x_b$, where x_a is less than x_b . The contribution to the total force coefficient C_{F_ℓ} at a given time, t , which results from the integration over this segment of the $(mn)^{th}$ pressure coefficient, can be obtained with the help of Fig. 10.



The numbered curves are the ones given in Fig. 9, except that now the circle is considered as two curves which meet at the point Q_2 . This point is at the intersection of the circle and a line of slope, R' , drawn tangent to the circle. The point Q_1 is at the intersection of curves 1 and 3 (and 2) and has the coordinates

$$x = \xi_n + \frac{\beta^2 U T_m}{M^2} \quad (9.3)$$

$$r = \frac{\beta U T_m}{M^2} \quad (9.4)$$

Through Q_1 is also drawn a line of slope R' . These two additional lines then help form the new regions labeled F, G, H, and I.

The line given in (9.2) intersects the curves 1, 2, 3, and 4 at the points

$$x_1 = \frac{\xi_n + \beta P}{1 - \beta R'} \quad (9.5)$$

$$x_3 = \frac{\xi_n + U T_m - P/\beta}{1 + R'/\beta} \quad (9.6)$$

$$x_{2,4} = \frac{\xi_n + U T_m - R'P}{1 + R'^2} \left\{ 1 \mp \sqrt{1 - \frac{(1 + R'^2) [P^2 + (\xi_n + U T_m)^2 - a^2 T_m^2]}{[\xi_n + U T_m - PR']^2}} \right\} \quad (9.7)$$

Equation (9.7) gives imaginary roots if there is no intersection. The end points of the line segment, (9.1), can easily be located relative to the regions shown in Fig. 10. Once this is done, Table I can be used as an aid in determining the limits of integration (values of x) to be used with the indefinite integrals given in Section VIII.

TABLE I

LIMITS FOR FORCE INTEGRALS

<u>Location of x_a</u>	<u>Location of x_b</u>	<u>Limits, Region B</u>		<u>Limits, Regions C and D</u>	
		<u>Lower</u>	<u>Upper</u>	<u>Lower</u>	<u>Upper</u>
A	A	-	-	-	-
A	B	x_1	x_b	-	-
A	C	x_1	x_2	x_2	x_b
A	D	x_1	x_2	x_2	x_b
A	E	x_1	x_2	x_2	x_4
B	B	x_a	x_b	-	-
B	C	x_a	x_2	x_2	x_b
B	D	x_a	x_2	x_2	x_b
B	E	x_a	x_2	x_2	x_4
C	C	-	-	x_a	x_b
C	D	-	-	x_a	x_b
C	E	-	-	x_a	x_4
D	D	-	-	x_a	x_b
D	E	-	-	x_a	x_4
E	E	-	-	-	-
A	F	-	-	-	-
A	G	-	-	x_2	x_b
A	H	-	-	x_2	x_4
F	F	-	-	-	-
F	G	-	-	x_2	x_b
F	H	-	-	x_2	x_4
G	G	-	-	x_a	x_b
G	H	-	-	x_a	x_4
H	H	-	-	-	-
A	I	-	-	-	-
I	I	-	-	-	-

Regions C and D are really no different as far as the force coefficients are concerned. There are also a few other ways that the table could be shortened; but since the use of a computer is assumed, it is easier to have a longer table utilizing simpler and more direct logic.

To obtain the total force coefficient, then, one needs only to repeat this procedure for all of the ξ_n and for all line segments such as (9.2). A double summation then yields the desired result.

X. CONCLUSIONS AND RECOMMENDATIONS

Two basic methods were considered for predicting indicial aerodynamic forces on cone-cylinder bodies of revolution. The Karman-Moore [1] technique uses a superposition idea well suited to digital computers, while the method of Adams and Sears [8] is more analytical in nature, using transforms and expansions about the slender body solution.

The Adams-Sears scheme is not so well adapted to handling slope discontinuities, so the Karman-Moore idea was considered to be more useful for this study.

A fundamental solution - the gust doublet - can be used with the Karman-Moore method for pointed bodies with arbitrary profiles. This solution is derivable from more elementary point sources by superposition. The gust doublet possesses certain properties in various regions of space:

1. An undisturbed region upstream of the Mach cone,
2. An undisturbed region sufficiently far downstream, into which the disturbance has yet to propagate,
3. A spherical region characterized by transient or unsteady flow, and
4. A region in which steady-state flow has been achieved.

It can be shown that the existence of these various regions is a property of general solutions to the unsteady potential equation.

The gust doublet satisfies the exact boundary condition for a cone in the steady-state region. Furthermore, the solution is precisely that of Tsien's in this region. Therefore, existing numerical procedures for computing steady crossflow, based on his modification of the Karman-Moore method, can be

readily extended to the indicial case. The boundary condition is satisfied in an approximate sense in the transient region by the gust doublet, and exactly when the limit of slender bodies is considered.

The work of Bond and Packard can be modified to yield a solution of the same form as the gust doublet, but with the wrong magnitude. The two theories agree, however, in the case of a body which is vanishingly thin.

The linearized lift coefficient differs in many ways from that of Miles for a cone. Miles' theory gives the slender body lift coefficient at steady state, whereas the present theory is "exact" as far as linear potential theory is concerned. The growth of lift for the gust doublet differs from Miles' result in the following respects:

1. It has no "overshoot."
2. It is a function of both M and R' , and not simply of the product MR' .
3. Its initial rate of growth is more rapid.
4. It has no discontinuities in the rate of growth of lift.
5. It reaches steady state in a finite time.

The inclusion of the quadratic terms in the pressure coefficient is necessary in order to obtain accurate force coefficients. One must retain those terms involving axial derivatives, and not just the radial derivatives, as is often done. This is particularly true with blunter bodies, and at Mach numbers significantly higher than 1.

The generalized force coefficients can be expressed in integral form. In special cases, the integrations can be carried out analytically, but in general, a numerical integration would probably be more efficient. More work should be done, both in obtaining the force coefficients as well as comparing them with other theories (e.g., steady nonlinear flow theory for cones). This is mandatory if one is to be able to establish ranges of applicability and accuracy of the gust doublet technique.

An exact solution for a cone encountering a step side gust, based on linearized potential theory, should be obtained. This would serve as a basis for comparison of approximate theories. An analytic solution seems improbable, but there are definite possibilities of obtaining numerical solutions. One possibility is the technique discussed in Appendix D. It should be pursued further in order to assure its convergence, etc. Modifications may be necessary to obtain high accuracy economically.

The idea of using surface source and doublet distributions is interesting from an intellectual viewpoint, but appears to be impractical due to the extreme complexity of the resulting mathematical forms. Unless some new insight is obtained from and about such a technique, it is recommended that it not be pursued further.

A more accurate theory for predicting the forces produced by an impulsive side wind would be highly desirable. The unit impulse is often the most convenient kernel to use in the Duhamel integral technique of computing missile responses to actual wind profiles. An impulse theory could be obtained either analytically or numerically from the existing gust doublet theory. The choice of a technique will involve a consideration of the economies involved, accuracy obtainable, and the form of the results.

BIBLIOGRAPHY

1. Von Karman, Th., and N. B. Moore, "Resistance of Slender Bodies Moving with with Supersonic Velocities, with Special Reference to Projectiles," Trans. A.S.M.E., 54, 303-310 (1932).
2. Tsien, H. S., "Supersonic Flow Over an Inclined Body of Revolution," J. Aero. Sci., 5, 480-483 (1938).
3. Lighthill, M. J., "Supersonic Flow Past Bodies of Revolution," Aero Res. Counc., R. and M. No. 2003, January, 1945.
4. Lighthill, M. J., "Supersonic Flow Past Slender Pointed Bodies of Revolution at Yaw," Quart. J. Mech. and Appl. Math., I, 76-89 (1948).
5. Ward, G. N., "Supersonic Flow Past Slender Pointed Bodies," Quart. J. Mech. and Appl. Math., Vol. II, Part 1, 75-97 (1949).
6. Broderick, J. B., "Supersonic Flow Round Pointed Bodies of Revolution," Quart. J. Mech. and Appl. Math., Vol. II, Part 1, 98-120 (1949).
7. Lighthill, M. J., "Supersonic Flow Past Slender Bodies of Revolution the Slope of Whose Meridian Section is Discontinuous," Quart. J. Mech. and Appl. Math., I, 90-102 (1948).
8. Adams, M. C., and W. R. Sears, "Slender Body Theory - Review and Extension," J. Aero. Sci., Vol. 20, No. 2, 85-98, February, 1953.
9. Li, Ta C. H., "Coupled Potential Flow Past Inclined Bodies of Revolution at High Speeds," Convair Astronautics, Rept. No. AZR-005 (1959).
10. Platzer, M. F., "Aerodynamic Pitch Damping of Slowly Oscillating Pointed Bodies of Revolution in Linearized Supersonic Flow," George C. Marshall Space Flight Center, MTP-AERO-63-62 (1963).
11. Dorrance, W. H., "Nonsteady Supersonic Flow," J. Aero Sci., 18, 501-511 (1951).
12. Lansing, D. L., "Velocity Potential and Forces on Oscillating Slender Bodies of Revolution in Supersonic Flow Expanded to the Fifth Power of the Frequency," NASA TN-D-1225 (1962).

13. Bond, R. B., and B. B. Packard, "Unsteady Aerodynamic Forces on a Slender Body of Revolution in Supersonic Flow," NASA, TN-D-859 (1961).
14. Zartarian, G., and H. Ashley, "Forces and Moments on Oscillating Slender Wing-Body Combinations at Supersonic Speed," AFOSR, TN 57-386 (1957).
15. Platzter, M. F., "A Note on the Solution for the Slowly Oscillating Body of Revolution in Supersonic Flow," George C. Marshall Space Flight Center, MTP-Aero-63-28 (1963).
16. Dzygadło, Z., "Linearized Supersonic Flow Past a Vibrating Surface of a Body of Revolution," Proc. of Vibration Problems, Vol. 2, No. 3 (8), 265-284, Warsaw (1961).
17. Miles, J. W., The Potential Theory of Unsteady Supersonic Flow, Cambridge University Press (1959).
18. Yates, J. E., "Research on the Loading of Missiles Due to Atmospheric Turbulence and Wind Shear, Transient Aerodynamic Loading on Multi-Stage Missiles," Title Unclassified, Phase Report, 23 August 1961 - 1 March 1962, Contract No. NAS8-2466, MRI Project No. 2544-P (Confidential).
19. Yates, J. E., "Transient Aerodynamic Loading on Multi-Stage Missiles," Paper presented at the IAS National Summer Meeting, Los Angeles, California, June 19-22, 1962, IAS Paper No. 62-93.
20. Blackburn, R. R., See Vol. II of this report.
21. Strang, W., "Transient Source, Doublet, and Vortex Solutions of the Linearized Equations of Supersonic Flow," Proc. Roy Soc. A, 202, 40-53 (1950).
22. Erdélyi, Magnus, Oberhettinger, and Tricomi, Tables of Integral Transforms, (Bateman Manuscript Project, California Inst. of Tech.), Vol. 1, 5.16 (47), 284, McGraw-Hill (1954).
23. Luke, Y. L., Integrals of Bessel Functions, 1.4.6 (8), 32, McGraw-Hill (1962).
24. Handbook of Mathematical Functions with Formulas, Graphs, and Mathematical Tables, Edited by M. Abramowitz, and I. A. Stegun, Nat. Bur. Standards, App. Math. Series, 55, Chapter 10, Formula 10.2.13 (1964).

25. See, for instance, the Princeton Series on "High Speed Aerodynamics and Jet Propulsion," Vol. VI, General Theory of High Speed Aerodynamics, Chapter 3, Part D, by M. A. Heaslet, and H. Lomax, edited by W. R. Sears (1954).
26. Gröbner, W., and N. Hofreiter, Integraltafel, Zweiter Teil, Bestimmte Integrale, 104, Springer-Verlag (1950).
27. Liepman, H. W., and A. Roshko, Elements of Gasdynamics, John Wiley and Sons (1957).
28. Lomax, H., "Indicial Aerodynamics," Chapter 6 of Vol. II, Manual on Aeroelasticity, AGARD.

APPENDIX A

REVIEW OF THE KARMAN-MOORE AND TSIENT THEORIES

Von Karman and Moore [1] developed a numerical method of solving for the steady axial flow over an arbitrary pointed body with axial symmetry. Later Tsien [2] used the same basic technique for the steady crossflow. This work will be reviewed briefly here since it is needed for the application of the gust doublet solution discussed elsewhere.

For steady axial flow, a basic solution is the source distribution given by

$$\phi(x, r) = \int_0^{x-\beta r} \frac{f(\xi) d\xi}{\sqrt{(x-\xi)^2 - \beta^2 r^2}} \quad (A.1)$$

The upper limit reflects the supersonic character of the solution, it being the equation of the Mach line. By choosing $f(\xi) = B\xi$, where B is a constant, the potential becomes

$$\phi = B \left\{ (x \cosh^{-1} \frac{x}{\beta r}) - \sqrt{x^2 - \beta^2 r^2} \right\} \quad (A.2)$$

This corresponds to conical flow. It represents a series of sources distributed along the positive x -axis, starting at the origin. The source strength is proportional to the distance from the origin.

A generalization of (A.2) is easily made by starting the source distribution at, say, $x = \xi_k$. Then,

$$\phi_k = B_k \left\{ (x - \xi_k) \cosh^{-1} \left(\frac{x - \xi_k}{\beta r} \right) - \sqrt{(x - \xi_k)^2 - \beta^2 r^2} \right\} \quad (A.3)$$

The corresponding velocity components are then

$$u_k = - B_k \cosh^{-1} \left(\frac{x - \xi_k}{\beta r} \right) \quad (A.3)$$

$$v_k = \beta B_k \sqrt{\left(\frac{x - \xi_k}{\beta r} \right)^2 - 1} \quad (A.5)$$

The numerical technique consists of summing a group of suitably chosen solutions of this form. This is facilitated by Fig. 11.

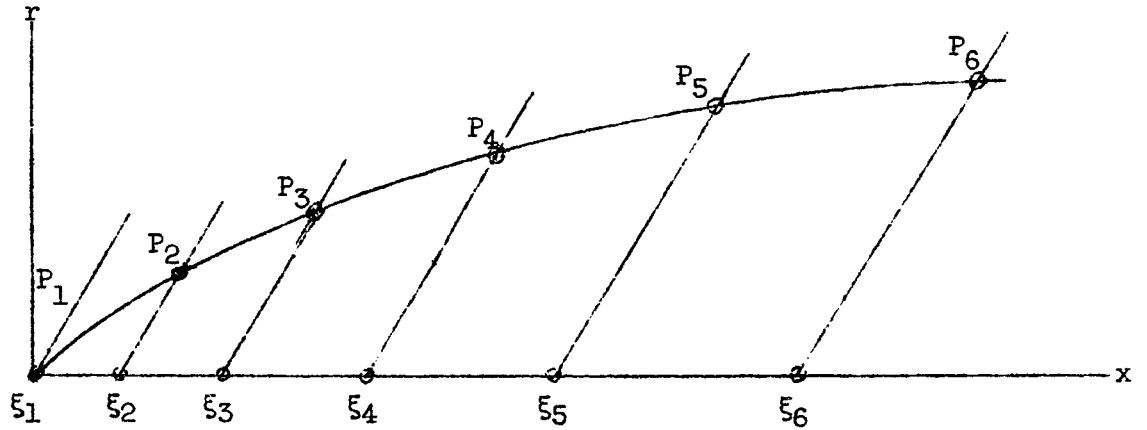


Fig. 11 - Control Points

The first step is to select a sequence of control points, P_k , on the surface of the body. Through these points are drawn Mach lines which intersect the x -axis at the points ξ_k . The velocities at a point, P_k , are then

$$u(x_k, r_k) = \sum_{i=1}^{k-1} B_i \left[\cosh^{-1} \left(\frac{x_k - \xi_{i+1}}{\beta r_k} \right) - \cosh^{-1} \left(\frac{x_k - \xi_i}{\beta r_k} \right) \right] \quad (A.6)$$

$$v(x_k, r_k) = - \beta \sum_{i=1}^{k-1} B_i \left[\sqrt{\left(\frac{x_k - \xi_{i+1}}{\beta r_k} \right)^2 - 1} - \sqrt{\left(\frac{x_k - \xi_i}{\beta r_k} \right)^2 - 1} \right] \quad (A.7)$$

The boundary condition

$$\left. \frac{dr}{dx} \right|_{\text{Body}} = \frac{v}{U + u} \quad (\text{A.8})$$

is then used to determine the B 's . If (A.8) is applied at P_2 , B_1 can be found. Then, B_2 can be determined by using the boundary condition at P_3 . The scheme can be continued in this manner until all the B 's are known.

The velocities at intermediate points can then be easily computed. For a point P which lies between P_k and P_{k+1} we have

$$u(x,r) = \sum_{i=1}^{k-1} B_i \left[\cosh^{-1} \left(\frac{x-\xi_{i+1}}{\beta r} \right) - \cosh^{-1} \left(\frac{x-\xi_i}{\beta r} \right) \right] - B_k \cosh^{-1} \left(\frac{x-\xi_k}{\beta r} \right) \quad (\text{A.9})$$

$$v(x,r) = -\beta \sum_{i=1}^{k-1} B_i \left[\sqrt{\left(\frac{x-\xi_{i+1}}{\beta r} \right)^2 - 1} - \sqrt{\left(\frac{x-\xi_i}{\beta r} \right)^2 - 1} \right] + \beta B_k \sqrt{\left(\frac{x-\xi_k}{\beta r} \right)^2 - 1} \quad (\text{A.10})$$

It is often more convenient to rearrange (A.9) and (A.10) so that they appear as

$$u(x,r) = -B_1 \cosh^{-1} \left(\frac{x-\xi_1}{\beta r} \right) - \sum_{i=2}^k (B_i - B_{i-1}) \cosh^{-1} \left(\frac{x-\xi_i}{\beta r} \right) \quad (\text{A.11})$$

$$v(x,r) = \beta B_1 \sqrt{\left(\frac{x-\xi_1}{\beta r} \right)^2 - 1} + \beta \sum_{i=2}^k (B_i - B_{i-1}) \sqrt{\left(\frac{x-\xi_i}{\beta r} \right)^2 - 1} \quad (\text{A.12})$$

The problem of steady crossflow may be handled in exactly the same fashion. Here, however, the basic potential function is

$$\phi_k = B_k \left\{ \beta^2 r \cosh^{-1} \left(\frac{x-\xi_k}{\beta r} \right) - (x-\xi_k) \sqrt{\left(\frac{x-\xi_k}{\beta r} \right)^2 - 1} \right\} \quad (A.13)$$

and the velocities are

$$u_k = 2B_k \beta \sqrt{\left(\frac{x-\xi_k}{\beta r} \right)^2 - 1} \quad (A.14)$$

$$v_k = -B_k \beta^2 \left\{ \cosh^{-1} \left(\frac{x-\xi_k}{\beta r} \right) + \frac{x-\xi_k}{\beta r} \sqrt{\left(\frac{x-\xi_k}{\beta r} \right)^2 - 1} \right\} \quad (A.15)$$

In this case, the boundary condition is

$$v - u \frac{dr}{dx} \Big|_{\text{Body}} = v_o \quad (A.16)$$

although Tsien used the slender body approximation

$$v = v_o \quad (A.17)$$

The technique presented here is quite general and can be applied readily to a variety of body shapes. Accuracy can be improved by using more control points. The manner of selecting the control points efficiently is largely a matter of experience. However, it can be said that generally one should choose these points closer together in regions of rapidly changing slope. For the case of a shoulder, several points should be located immediately downstream of the discontinuity to obtain the best accuracy.

APPENDIX B

THE USE OF SURFACE SOURCE DISTRIBUTIONS

This Appendix contains a treatment of the axial flow over bodies of revolution. A distribution of sources over the surface of the body is considered rather than an axial distribution of sources as in the Karman-Moore procedure. The steady flow case is considered. This was done in an effort to see what forms the solutions take.

The principal results are formulas (B.19a) and (B.19b) for the axial flow potential. They are integral expressions containing the elliptic integrals of the second kind. In the work immediately following (B.19a) and (B.19b) an attempt was made to satisfy the boundary conditions on the body surface. The resultant expressions became rather unwieldy. Finally, the special case of a cone in axial flow was considered. The final result for the cone is contained in Eq. (B.28). It is found that the cone problem can be solved with a surface distribution.

Consider the problem of axial flow over a body of revolution, as shown in Fig. 12.

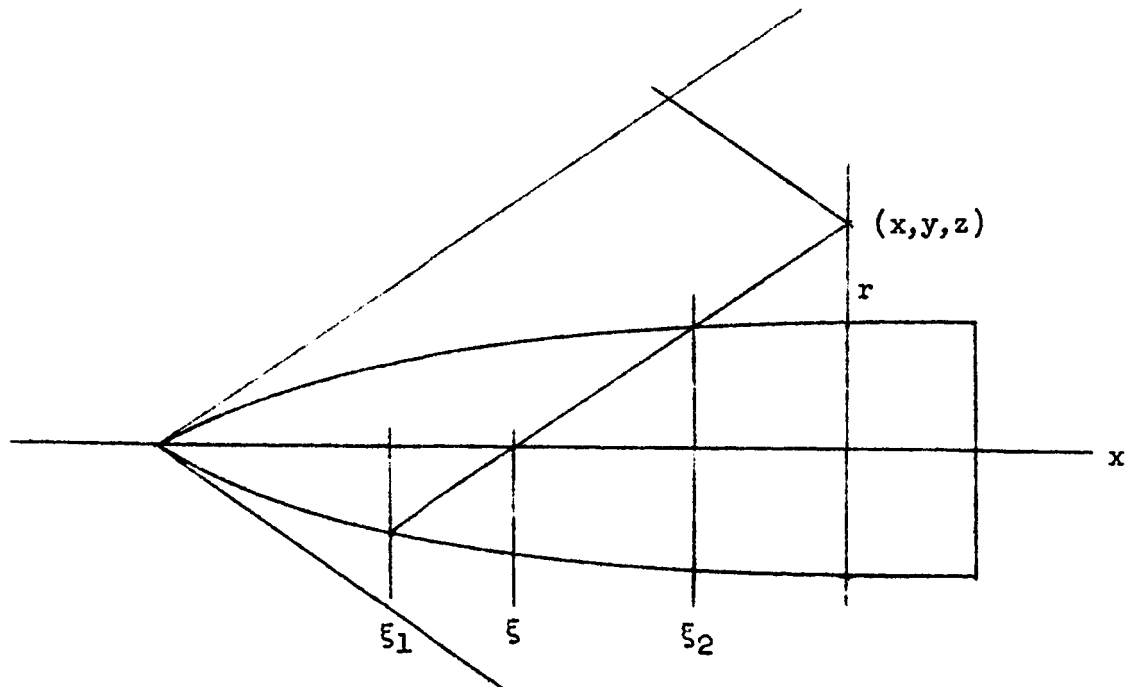


Fig. 12 - Notation for Appendix B

The axial flow equation is

$$\beta^2 \frac{\partial^2 \Phi}{\partial x^2} - \frac{\partial^2 \Phi}{\partial r^2} - \frac{1}{r} \frac{\partial \Phi}{\partial r} = 0 \quad (\text{B.1})$$

or

$$\beta^2 \frac{\partial^2 \Phi}{\partial x^2} - \frac{\partial^2 \Phi}{\partial y^2} - \frac{\partial^2 \Phi}{\partial z^2} = 0 \quad (\text{B.2})$$

while the boundary condition at the body is

$$\left[\frac{\partial \Phi}{\partial r} - R'(x) \frac{\partial \Phi}{\partial x} \right]_{r=R(x)} = R' \quad (\text{B.3})$$

Consider the basic source solution

$$\phi = \frac{1}{\sqrt{(x-\xi)^2 - \beta^2[(y-\eta)^2 + (z-\zeta)^2]}} = \frac{1}{\bar{r}} \quad (\text{B.4})$$

The characteristic cone opening forward from the point x, y, z is defined by $\bar{r} = 0$ or

$$(x-\xi)^2 - \beta^2[(y-\eta)^2 + (z-\zeta)^2] = 0 \quad (\text{B.5})$$

The body surface in coordinates ξ, η, ζ is

$$\eta^2 + \zeta^2 = R^2(\xi)$$

or

$$\begin{aligned}\eta &= R \sin \theta \\ \zeta &= R \cos \theta\end{aligned}\tag{B.6}$$

where $\theta = 0$ in the plane $y = 0$.

We want to construct a solution by placing sources on the body surface rather than along the axis. Defining the region of integration is the next step to be performed. Letting

$$\begin{aligned}y &= r \sin \psi \\ z &= r \cos \psi\end{aligned}$$

we have, using (B.6),

$$(y-\eta)^2 + (z-\zeta)^2 = r^2 + R^2 - 2Rr \cos (\theta-\psi) \quad . \tag{B.7}$$

But we shall perform an integration on θ symmetric in ψ . Hence we can take $\psi = 0$ in (B.7) without loss of generality. We write

$$\phi = \frac{1}{\sqrt{(x-\xi)^2 - \beta^2(r^2 - 2Rr \cos \theta + R^2)}} \tag{B.8}$$

where $R = R(\xi)$

The solution desired can be written in the form

$$\begin{aligned}
\Phi = & \int_0^{\xi_1} \int_{-\pi}^{\pi} \frac{f(\xi) d\theta d\xi}{\sqrt{(x-\xi)^2 - \beta^2(r^2 - 2Rr \cos \theta + R^2)}} \\
& + \int_{\xi_1}^{\xi_2} \int_{-\theta_0}^{\theta_0} \frac{f(\xi) d\theta d\xi}{\sqrt{(x-\xi)^2 - \beta^2(r^2 - 2Rr \cos \theta + R^2)}}
\end{aligned} \tag{B.9}$$

where the limits of integration are the solutions of

$$\left. \begin{aligned} \xi_1 + \beta R(\xi_1) &= x - \beta r \\ \xi_2 - \beta R(\xi_2) &= x - \beta r \end{aligned} \right\} \tag{B.10}$$

and where

$$\theta_0 = \cos^{-1} \left\{ \frac{1}{2Rr} \left[r^2 + R^2 - \frac{(x-\xi)^2}{\beta^2} \right] \right\}, \quad 0 \leq \theta_0 \leq \pi \quad . \tag{B.11}$$

For the special case of the cone, (B.10) yields simply

$$\left. \begin{aligned} \xi_1 &= \frac{x - \beta r}{1 + \beta \delta} \\ \xi_2 &= \frac{x - \beta r}{1 - \beta \delta} \end{aligned} \right\}, \tag{B.12}$$

δ being the slope of the cone.

Since the arguments of (B.9) are even in θ , we write

$$\Phi = 2(\Phi_0 + \Phi_1) \tag{B.13}$$

where

$$\Phi_0 = \int_0^{\xi_1} \int_0^{\pi} \frac{f(\xi) d\theta d\xi}{\sqrt{(x-\xi)^2 - \beta^2(r^2 - 2Rr \cos \theta + R^2)}} \quad (\text{B.14})$$

$$\Phi_1 = \int_{\xi_1}^{\xi_2} \int_0^{\theta_0} \frac{f(\xi) d\theta d\xi}{\sqrt{(x-\xi)^2 - \beta^2(r^2 - 2Rr \cos \theta + R^2)}} \quad (\text{B.15})$$

Now, it can be shown that the integral

$$\int_0^{\theta_0} \frac{d\theta}{\sqrt{a+b \cos \theta}} = \sqrt{\frac{2}{b}} K\left(\sqrt{\frac{a+b}{2b}}\right) \quad (\text{B.16})$$

where $\theta_0 = \cos^{-1}\left(-\frac{a}{b}\right)$ and K here is the complete elliptic integral of the first kind. Also, we have [26]

$$\int_0^{\pi} \frac{d\theta}{\sqrt{a+b \cos \theta}} = \frac{2}{\sqrt{a+b}} K\sqrt{\frac{2b}{a+b}} \quad (\text{B.17})$$

Using the relations

$$\left. \begin{aligned} a &= (x-\xi)^2 - \beta^2(r^2 + R^2) \\ b &= 2\beta^2 Rr \end{aligned} \right\} \quad (\text{B.18})$$

one then obtains

$$\phi_0 = \int_0^{\xi_1} \frac{2f(\xi)}{\sqrt{(x-\xi)^2 - \beta^2(r-R)^2}} K \left(\sqrt{\frac{4\beta^2 Rr}{(x-\xi)^2 - \beta^2(r-R)^2}} \right) d\xi \quad (\text{B.19a})$$

$$\phi_1 = \int_{\xi_1}^{\xi_2} \frac{2f(\xi)}{\sqrt{4\beta^2 Rr}} K \left(\sqrt{\frac{(x-\xi)^2 - \beta^2(r-R)^2}{4\beta^2 Rr}} \right) d\xi \quad (\text{B.19b})$$

where, in general, $R = R(\xi)$.

It remains now to apply the boundary conditions (B.3) at the surface of the body.

Note that the integrals in (B.19a) and (B.19b) are singular; i.e., $K(k) \rightarrow \infty$ as $k \rightarrow 1$ or $\xi \rightarrow \xi_1$. However, the integrals of these terms yield a finite result.

The forms (B.19a) and (B.19b) are not as unappealing as they may look. The expression simplifies somewhat when the boundary condition is applied. Take x and r derivatives of (B.19a) and (B.19b). After much manipulation, one obtains

$$\begin{aligned} \frac{\partial \phi_0}{\partial x} = & - \int_0^{\xi_1} \frac{2f(\xi)(x-\xi)}{[(x-\xi)^2 - \beta^2(r-R)^2]^{3/2}} K \left(\sqrt{\frac{4\beta^2 Rr}{(x-\xi)^2 - \beta^2(r-R)^2}} \right) d\xi \\ & - \int_0^{\xi_1} \frac{2f(\xi) \sqrt{4\beta^2 Rr} (x-\xi)}{[(x-\xi)^2 - \beta^2(r-R)^2]^2} K' \left(\sqrt{\frac{4\beta^2 Rr}{(x-\xi)^2 - \beta^2(r-R)^2}} \right) d\xi \\ & + \left(\frac{\partial \xi_1}{\partial x} \right) \left\{ \frac{2f(\xi)}{\sqrt{(x-\xi)^2 - \beta^2(r-R)^2}} K \left(\sqrt{\frac{4\beta^2 Rr}{(x-\xi)^2 - \beta^2(r-R)^2}} \right) \right\}_{\xi = \xi_1(x,r)} . \end{aligned} \quad (\text{B.20})$$

$$\begin{aligned}
\frac{\partial \phi_0}{\partial r} = & \int_0^{\xi_1} \frac{2f(\xi)\beta^2(r-R)}{[(x-\xi)^2 - \beta^2(r-R)^2]^{3/2}} K \left(\sqrt{\frac{4\beta^2 Rr}{(x-\xi)^2 - \beta^2(r-R)^2}} \right) d\xi \\
& + \int_0^{\xi_1} \left\{ \frac{2f(\xi) \sqrt{4\beta^2 Rr} \beta^2(r-R)}{[(x-\xi)^2 - \beta^2(r-R)^2]^2} + \frac{4f(\xi)\beta^2 R}{\sqrt{4\beta^2 Rr} [(x-\xi)^2 - \beta^2(r-R)^2]} \right\} \\
& \times K' \left(\sqrt{\frac{4\beta^2 Rr}{(x-\xi)^2 - \beta^2(r-R)^2}} \right) d\xi \\
& + \left(\frac{\partial \xi_1}{\partial r} \right) \left\{ \frac{2f(\xi)}{\sqrt{(x-\xi)^2 - \beta^2(r-R)}} K \left(\sqrt{\frac{4\beta^2 Rr}{(x-\xi)^2 - \beta^2(r-R)^2}} \right) \right\}_{\xi = \xi_1(x,r)}
\end{aligned}
\tag{B.21}$$

$$\begin{aligned}
\frac{\partial \phi_1}{\partial x} = & \int_{\xi_1}^{\xi_2} \frac{2f(\xi)(x-\xi)}{4\beta^2 Rr [(x-\xi)^2 - \beta^2(r-R)^2]^{1/2}} K' \left(\sqrt{\frac{(x-\xi)^2 - \beta^2(r-R)^2}{4\beta^2 Rr}} \right) d\xi \\
& + \left(\frac{\partial \xi_2}{\partial x} \right) \left\{ \frac{2f(\xi)}{\sqrt{4\beta^2 Rr}} K \left(\sqrt{\frac{(x-\xi)^2 - \beta^2(r-R)^2}{4\beta^2 Rr}} \right) \right\}_{\xi = \xi_2(x,r)} \\
& - \left(\frac{\partial \xi_1}{\partial x} \right) \left\{ \frac{2f(\xi)}{\sqrt{4\beta^2 Rr}} K \left(\sqrt{\frac{(x-\xi)^2 - \beta^2(r-R)^2}{4\beta^2 Rr}} \right) \right\}_{\xi = \xi_1(x,r)} .
\end{aligned}
\tag{B.22}$$

$$\begin{aligned}
\frac{\partial \phi_1}{\partial r} = & - \int_{\xi_1}^{\xi_2} \frac{4f(\xi)\beta^2 R}{(4\beta^2 Rr)^{3/2}} K \left(\sqrt{\frac{(x-\xi)^2 - \beta^2(r-R)^2}{4\beta^2 Rr}} \right) d\xi \\
& - \int_{\xi_1}^{\xi_2} \left\{ \frac{2f(\xi)\beta^2(r-R)}{4\beta^2 Rr [(x-\xi)^2 - \beta^2(r-R)^2]^{1/2}} + \frac{4f(\xi)\beta^2 R [(x-\xi)^2 - \beta^2(r-R)^2]^{1/2}}{(4\beta^2 Rr)^2} \right\} \\
& \times K' \left(\sqrt{\frac{(x-\xi)^2 - \beta^2(r-R)^2}{4\beta^2 Rr}} \right) d\xi \\
& + \left(\frac{\partial \xi_2}{\partial r} \right) \left\{ \frac{2f(\xi)}{\sqrt{4\beta^2 Rr}} K \left(\sqrt{\frac{(x-\xi)^2 - \beta^2(r-R)^2}{4\beta^2 Rr}} \right) \right\}_{\xi = \xi_2(x,r)} \\
& - \left(\frac{\partial \xi_1}{\partial r} \right) \left\{ \frac{2f(\xi)}{\sqrt{4\beta^2 Rr}} K \left(\sqrt{\frac{(x-\xi)^2 - \beta^2(r-R)^2}{4\beta^2 Rr}} \right) \right\}_{\xi = \xi_1(x,r)} \tag{B.23}
\end{aligned}$$

Combining (B.20) and (B.22), and (B.21) and (B.23), the singular terms at ξ_1 cancel. Furthermore, at ξ_2 the argument of K goes to zero and

$$K(0) = \pi/2 \tag{B.24}$$

Thus, combining (B.20) and (B.22) we get

$$\begin{aligned}
\frac{\partial \phi_0}{\partial x} + \frac{\partial \phi_1}{\partial x} = & - \int_0^{\xi_1} \frac{2f(\xi)(x-\xi)}{[(x-\xi)^2 - \beta^2(r-R)^2]^{3/2}} K \left(\sqrt{\frac{4\beta^2 Rr}{(x-\xi)^2 - \beta^2(r-R)^2}} \right) d\xi \\
& - \int_0^{\xi_1} \frac{2f(\xi) \sqrt{4\beta^2 Rr} (x-\xi)}{[(x-\xi)^2 - \beta^2(r-R)^2]^2} K' \left(\sqrt{\frac{4\beta^2 Rr}{(x-\xi)^2 - \beta^2(r-R)^2}} \right) d\xi \\
& + \int_{\xi_1}^{\xi_2} \frac{2f(\xi)(x-\xi)}{4\beta^2 Rr [(x-\xi)^2 - \beta^2(r-R)^2]^{1/2}} K' \left(\sqrt{\frac{(x-\xi)^2 - \beta^2(r-R)^2}{4\beta^2 Rr}} \right) d\xi \\
& + \left(\frac{\partial \xi_2}{\partial x} \right) \left[\frac{\pi f(\xi)}{\sqrt{4\beta^2 Rr}} \right]_{\xi = \xi_2} = \xi_2(x, r)
\end{aligned} \tag{B.25}$$

Combining (B.21) and (B.23) we get

$$\begin{aligned}
\frac{\partial \xi_0}{\partial r} + \frac{\partial \xi_1}{\partial r} = & \int_0^{\xi_1} \frac{2f(\xi)\beta^2(r-R)}{[(x-\xi)^2 - \beta^2(r-R)^2]^{3/2}} K \left(\sqrt{\frac{4\beta^2 Rr}{(x-\xi)^2 - \beta^2(r-R)^2}} \right) d\xi \\
& + \int_0^{\xi_1} \left\{ \frac{2f(\xi) \sqrt{4\beta^2 Rr} \beta^2(r-R)}{[(x-\xi)^2 - \beta^2(r-R)^2]^2} + \frac{4f(\xi)\beta^2 R}{\sqrt{4\beta^2 Rr} [(x-\xi)^2 - \beta^2(r-R)^2]} \right\} \\
& \times K' \left(\sqrt{\frac{4\beta^2 Rr}{(x-\xi)^2 - \beta^2(r-R)^2}} \right) d\xi \\
& - \int_{\xi_1}^{\xi_2} \frac{4f(\xi)\beta^2 R}{(4\beta^2 Rr)^{3/2}} K \left(\sqrt{\frac{(x-\xi)^2 - \beta^2(r-R)^2}{4\beta^2 Rr}} \right) d\xi \\
& - \int_{\xi_1}^{\xi_2} \left\{ \frac{2f(\xi)\beta^2(r-R)}{4\beta^2 Rr [(x-\xi)^2 - \beta^2(r-R)^2]^{1/2}} + \frac{4f(\xi)\beta^2 R [(x-\xi)^2 - \beta^2(r-R)^2]^{1/2}}{(4\beta^2 Rr)^2} \right\} \\
& \times K' \left(\sqrt{\frac{(x-\xi)^2 - \beta^2(r-R)^2}{4\beta^2 Rr}} \right) d\xi \\
& + \left(\frac{\partial \xi_2}{\partial r} \right) \left[\frac{\pi f(\xi)}{\sqrt{4\beta^2 Rr}} \right]_{\xi = \xi_2(x,r)}
\end{aligned} \tag{B.26}$$

From the appearance of (B.25) and (B.26), this method of solution does not, at first glance, look too appealing. However, it might be instructive to look at the solution for the pure cone in which case the various expressions simplify somewhat. We evaluate (B.25) and (B.26) on the surface of the body where

$$r = R(x) = \delta x \quad (\text{B.27})$$

Letting

$$\alpha^2 = (1 - \beta^2 \delta^2)$$

and applying (B.3), we find

$$\begin{aligned} & \left[\left(\frac{\partial \phi_0}{\partial r} + \frac{\partial \phi_1}{\partial r} \right)_{r=R(x)} - \delta \left(\frac{\partial \phi_0}{\partial x} + \frac{\partial \phi_1}{\partial x} \right)_{r=R(x)} \right] \\ &= \int_0^{\left(\frac{1-\beta\delta}{1+\beta\delta} \right) x} \frac{2\delta M^2}{\alpha^3} \frac{f(\xi)}{(x-\xi)^2} K \left(\frac{2\beta\delta}{\alpha} \frac{\sqrt{x\xi}}{(x-\xi)} \right) d\xi \\ &+ \int_0^{\left(\frac{1-\beta\delta}{1+\beta\delta} \right) x} \left\{ \frac{4\delta^2 \beta M^2}{\alpha^4} \frac{f(\xi)}{(x-\xi)^3} \frac{\sqrt{x\xi}}{(x-\xi)} + \frac{2\beta}{\alpha^2} \frac{f(\xi)\xi}{\sqrt{x\xi}(x-\xi)^2} \right\} K' \left(\frac{2\beta\delta}{\alpha} \frac{\sqrt{x\xi}}{(x-\xi)} \right) d\xi \\ &- \int_{\left(\frac{1-\beta\delta}{1+\beta\delta} \right) x}^x \left\{ \frac{M^2}{2\beta^2 \delta \alpha} \frac{f(\xi)}{x\xi} + \frac{\alpha}{4\beta^2 \delta^3} \frac{f(\xi)(x-\xi)}{x^2 \xi} \right\} K' \left(\frac{\alpha}{2\beta\delta} \frac{(x-\xi)}{\sqrt{x\xi}} \right) d\xi \\ &- \int_{\left(\frac{1-\beta\delta}{1+\beta\delta} \right) x}^x \frac{1}{2\beta\delta^2} \frac{f(\xi)\xi}{(x\xi)^{3/2}} K \left(\frac{\alpha}{2\beta\delta} \frac{(x-\xi)}{\sqrt{x\xi}} \right) d\xi \\ &- \frac{\pi(\beta+\delta)}{2\beta\delta(1-\beta\delta)} \frac{f(x)}{x} = \delta \end{aligned} \quad (\text{B.28})$$

If $f(x)$ is assumed to be linear in its argument and one makes the transformation $\xi = xy$ in the integral term of (B.28), the left hand side reduces to a constant. Thus, the boundary condition can be satisfied exactly for the cone. The surface source distribution has the same form as the line source distribution in the Karman-Moore procedure.

The case of steady crossflow can be attacked in much the same manner as presented here. The analysis is slightly more involved, with elliptic integrals of the first and second kinds involved.

Due to the complexity of the surface source distribution technique, it is not deemed advisable to use this method unless some distinct advantage over the axial source distribution is apparent. This is particularly true when one considers the extension to the non-steady problem.

APPENDIX C

APPLICATION OF BOND-PACKARD THEORY

The work of Bond and Packard [13] can be modified and extended to yield results which are similar in form to those presented in Section VII. Their work will be reviewed briefly here for completeness. Then, the appropriate downwash is inserted and the potential is obtained in closed form, for a conical body.

In terms of real time, t , the potential Eq. (3.1) may be written

$$-\beta^2 \phi_{xx} + \phi_{rr} + \frac{1}{r} \phi_r + \frac{1}{r^2} \phi_{\theta\theta} - \frac{2U}{a^2} \phi_{xt} - \frac{1}{a^2} \phi_{tt} = 0. \quad (C.1)$$

Bond and Packard used the approximate boundary condition

$$\phi_r \Big|_{r=R(x)} = W(x, t) \cos \theta$$

or, for the gust loading,

$$\phi_r \Big|_{r=R(x)} = v_0 \cos \theta H(Ut-x). \quad (C.2)$$

Assuming a $\cos \theta$ dependence of ϕ on θ , and taking the Laplace transform on t gives

$$-\beta^2 \bar{\phi}_{xx} + \bar{\phi}_{rr} + \frac{1}{r} \bar{\phi}_r - \frac{1}{r^2} \bar{\phi} - \frac{2Us}{a^2} \bar{\phi}_x - \frac{s^2}{a^2} \bar{\phi} = 0$$

with

$$\bar{\phi}_r \Big|_{r=R(x)} = \bar{W}(x, s) \quad (C.3)$$

where

$$\bar{\phi} = \frac{1}{\cos \theta} L(\phi) .$$

Transforming again on x and solving the resulting equation yields

$$\bar{\phi}(p, r, s) = f(p) K_1(\sigma r) \quad (C.4)$$

where

$$\sigma = \sqrt{\beta^2 p^2 + 2 \frac{U s p}{a^2} + \frac{s^2}{a^2}}$$

and $f(p)$ is an arbitrary function to be determined by the condition (C.3).

Since (C.3) cannot be transformed on x , the function $\bar{\phi}$ is written as

$$\bar{\phi} = \frac{1}{2\pi i} \int_{c-i\infty}^{c+i\infty} e^{px} f(p) K_1(\sigma r) dp \quad (C.5)$$

The slender body approximation is made here by writing

$$K_1(\sigma r) \approx \frac{1}{\sigma r} \quad (C.6)$$

This allows the r -dependence to be separated out. Using (C.6) and (C.5) in (C.3) results in

$$\frac{1}{2\pi i} \int_{c-i\infty}^{c+i\infty} \frac{e^{px} f(p) dp}{\sigma} = - R^2(x) \bar{W}(x, s) \quad (C.7)$$

Then, taking the Laplace transform of (C.7), we can solve for $f(p)$ to obtain

$$\frac{f(p)}{\sigma} = - \int_0^\infty e^{-p\xi} R^2(\xi) \bar{W}(\xi, s) d\xi \quad (C.8)$$

This expression is placed in (C.5). Now, the approximation (C.6) is not used for $K_1(\text{or})$ in (C.5). Rather, it is possible to rewrite (C.5) in terms of the convolution integral

$$\bar{\phi}(x, r, s) = \frac{\partial}{\partial r} \int_0^\infty e^{-\frac{Ms}{\beta^2 a} (x-\xi)} \frac{\cosh \left[\frac{s}{\beta^2 a} \sqrt{(x-\xi)^2 - \beta^2 r^2} \right] R^2(\xi) \bar{W}(\xi, s)}{\sqrt{(x-\xi)^2 - \beta^2 r^2}} d\xi \quad (\text{C.9})$$

where, to keep the integrand real, we require $\xi \leq x - \beta r$.

Now,

$$\bar{W}(\xi, s) = \frac{1}{s} e^{-\frac{s\xi}{U}} v_0 \quad (\text{C.10})$$

We put (C.10) in (C.9), take the inverse transform of (C.9) and interchange the order of integration to obtain

$$\phi(x, r, t) = \frac{\partial}{\partial r} \int_0^{x-\beta r} \frac{R^2(\xi) v_0}{\sqrt{(x-\xi)^2 - \beta^2 r^2}} \times \left\{ \frac{1}{2\pi i} \int_{c-i\infty}^{c+i\infty} e^{s(t - \frac{M}{\beta^2 a} (x-\xi) - \xi/U)} \cosh \left[\frac{s}{\beta^2 a} \sqrt{(x-\xi)^2 - \beta^2 r^2} \right] \frac{ds}{s} \right\} d\xi \cos \theta \quad (\text{C.11})$$

Expressing the cosh in terms of exponentials, the quantity in brackets may be written

$$\frac{1}{2\pi i} \int_{c-i\infty}^{c+i\infty} e^{\frac{s(t-\tau_1)}{2s}} + e^{\frac{s(t-\tau_2)}{2s}} ds \quad (\text{C.12})$$

where

$$\tau_{1,2} = \frac{M}{\beta^2 a} (x - \xi) + \frac{\xi}{U} \pm \frac{1}{\beta^2 a} \sqrt{(x - \xi)^2 - \beta^2 r^2} \quad (C.13)$$

The expression (C.12) may be immediately evaluated to give

$$\frac{1}{2} \left\{ H(t - \tau_1) + H(t - \tau_2) \right\} \quad (C.14)$$

Equation (C.11) hence becomes

$$\phi(x, r, t) = \frac{\partial}{\partial r} \int_0^{x - \beta r} \frac{v_0 R^2(\xi) [H(t - \tau_1) + H(t - \tau_2)] d\xi}{2 \sqrt{(x - \xi)^2 - \beta^2 r^2}} \cos \theta \quad (C.15)$$

Now, the quantities $t - \tau_1$ and $t - \tau_2$, together with the upper limit, are precisely the surfaces dividing the Regions A, B, C, D, and E. Therefore, the integration required in (C.15) is precisely of the same form as (7.1) if $R(\xi)$ describes a conical surface.

The resulting potential is identical to that found in Section VII except for a multiplying factor. That is, the solution obtained from (C.15) must be multiplied by the quantity

$$\frac{1}{\beta^2 R'^2 \cosh^{-1} \left(\frac{1}{\beta R'} \right) + \sqrt{1 - \beta^2 R'^2} (1 + 2R'^2)} \quad (C.16)$$

The expression (C.16) approaches 1 as R' approaches zero. In the limit of very slender bodies, then, the results from Bond and Packard agree with those of Section VII. However, for the steady-state portion, the gust doublet gives the exact results, whereas Bond and Packard's theory is only approximate. For this reason, it seems that the present theory may be more accurate generally.

Apparently, there is no easy way to relax the slender body approximation inherent in Eq. (C.6). Carrying additional terms in the series expansion for the Bessel function will not allow the separation accomplished in (C.7).

APPENDIX D

A NUMERICAL APPROACH TO THE INDICIAL AERODYNAMICS

The gust doublet solution given in Section IX satisfies the exact steady-state boundary condition for a cone. The boundary condition is satisfied only approximately in the region near the gust front, however. This approximation becomes better as the cone gets thinner - implying a slender body approximation.

In order to have a basis for comparison of the doublet solution with other approximations, it is desirable to have an exact solution. This Appendix outlines an approach to an exact numerical solution for a cone encountering a step gust.

The technique to be used here is an extension and generalization of the Karman-Moore technique into a second dimension, time. A series of fundamental solutions are to be chosen. These solutions will have two parameters, ξ_n , referring to a position on the x-axis, and a time origin, t_m . Each solution will have an unknown coefficient, A_{mn} , associated with it. Once the "layout" of these solutions in time and space is chosen, the boundary condition can be applied at various positions and times to determine the coefficients. Then, of course, any other desired quantities such as the lift coefficient can be found by summation.

The fundamental solution chosen should have certain properties. It should be time dependent, continuous, and finite everywhere. Based on these premises, the gust doublet solution is satisfactory for this purpose. In addition, it gives the steady-state solution exactly, which will aid in the judgment of convergence.

The values, ξ_n , are assumed to be equally spaced along the x-axis. The points, P_n , are then also equally spaced on the cone surface. To retain as much generality as is possible, it is assumed that at $t = 0$, all gust doublets start emitting. Then, at a time Δt later, another set of gust doublets at the points ξ_n start emitting. This set has $t_m = t_2 = \Delta t$. This procedure is then repeated with $t_3 = 2\Delta t$, etc. Thus, the coefficient A_{mn} is associated with a gust doublet located at ξ_n which starts emitting at t_m and whose Mach line passes through the point P_n on the surface. If there are N values of ξ and P , such that P_N is located at $x = 1$, $r = R'$, then,

$$P_n = \left(\frac{n-1}{N-1}, \frac{n-1}{N-1} R' \right) \quad (D.1)$$

$$\xi_n = \frac{n-1}{N-1} (1 - \rho R') \quad (D.2)$$

$$t_m = (m-1) \Delta t \quad (D.3)$$

See Fig. 13.

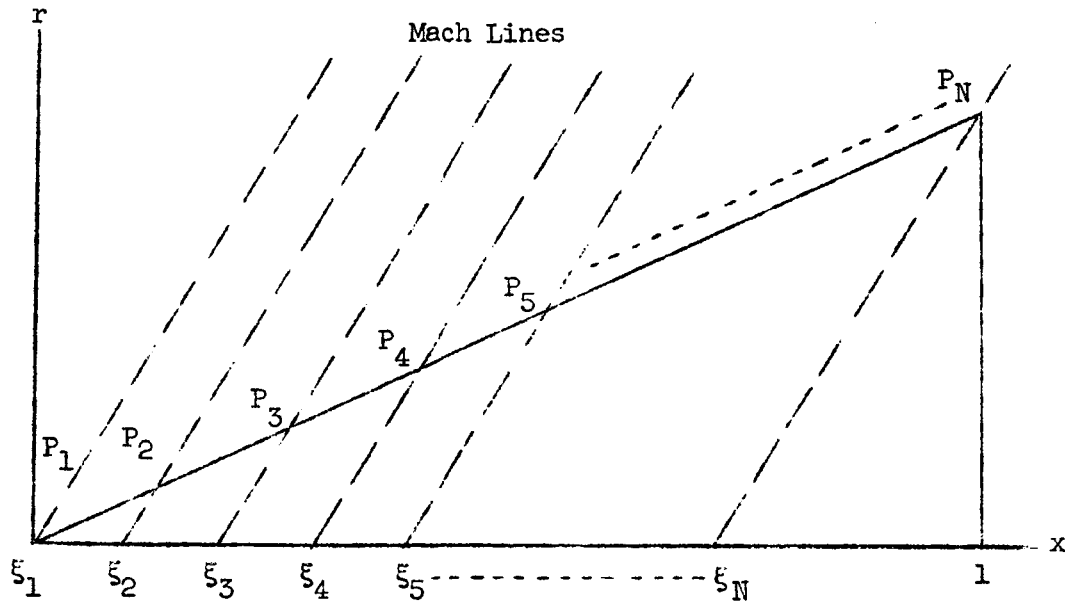


Fig. 13 - Location of Doublet Distributions

The main task now is to solve for the A_{mn} . The boundary condition can be applied $m \times n$ times to yield $m \times n$ equations for the coefficients. It is desirable to develop a relatively simple set of equations, to facilitate their solutions. For this reason, the points, P_n , themselves will be used as control points. The equation at the point, P_n , will involve only those A_{mi} which have $i < n$.

The time at which the boundary condition is to be satisfied must also be determined. If the time is too large, steady state will already have been attained. This, in turn, will lead to the relatively useless result that all A_{mn} are zero except A_{11} . The other extreme, that of using small times, leads to a divergence in the series of the A_{mn} .

The scheme presently being used is best explained as follows: Let l_1 be the time lag required for the value of $v - R'u$ at point P_2 , due to the potential at ξ_1 , to reach z per cent of its steady-state value. Likewise, l_n is the time lag associated with the value of $v - R'u$ at P_{n+1} , due to the potential at ξ_n . The solution for the A_{mn} is obtained by satisfying the boundary conditions at the points and times shown in Table II.

TABLE II
METHOD OF DETERMINING A_{mn}

<u>Point</u>	<u>Time</u>	<u>A_{mn} Solved For</u>
P_2	l_1	A_{11}
P_3	l_2	A_{12}
P_4	l_3	A_{13}
.	.	.
.	.	.
.	.	.
P_N	l_{N-1}	$A_{1\ N-1}$
P_2	$\Delta t + l_1$	A_{21}
P_3	$\Delta t + l_2$	A_{22}
P_4	$\Delta t + l_3$	A_{23}
.	.	.
.	.	.
.	.	.
P_N	$\Delta t + l_{N-1}$	$A_{2\ N-1}$
P_2	$2\Delta t + l_1$	A_{31}
.	.	.
.	.	.
.	.	.

The method described above has been programmed and the program has been debugged. Only a few preliminary results have been obtained. Table III shows the A_{mn} for a cone of unit length, slope = 0.15, at Mach number 2. The values $N = 5$ and $z = 80$ were used here, and the value of $U\Delta t$ was 0.2. The linearized lift coefficient is shown in Fig. 14.

The numerical solution appears to have the oscillatory characteristics of a Fourier series. If more terms are used, higher frequency oscillations can be expected. It is felt that more work is required before definitive results and conclusions can be given regarding this technique.

TABLE III

A_{mn} VALUES

<u>m</u>	<u>$A_{m1}/(v_o/U)$</u>	<u>$A_{m2}/(v_o/U)$</u>	<u>$A_{m3}/(v_o/U)$</u>	<u>$A_{m4}/(v_o/U)$</u>
1	0.30656	- 0.00070	0.00003	- 0.00001
2	- 0.07426	- 0.17868	- 0.16574	0.02811
3	0.01799	0.26746	0.41781	0.65727
4	- 0.00436	- 0.12055	- 0.46862	- 1.03315
5	0.00106	0.04312	0.33331	0.66150
6	- 0.00026	- 0.01391	- 0.16724	- 0.53563
7	0.00006	0.00424	0.06969	0.34352
8	- 0.00001	- 0.00124	- 0.02599	- 0.17766

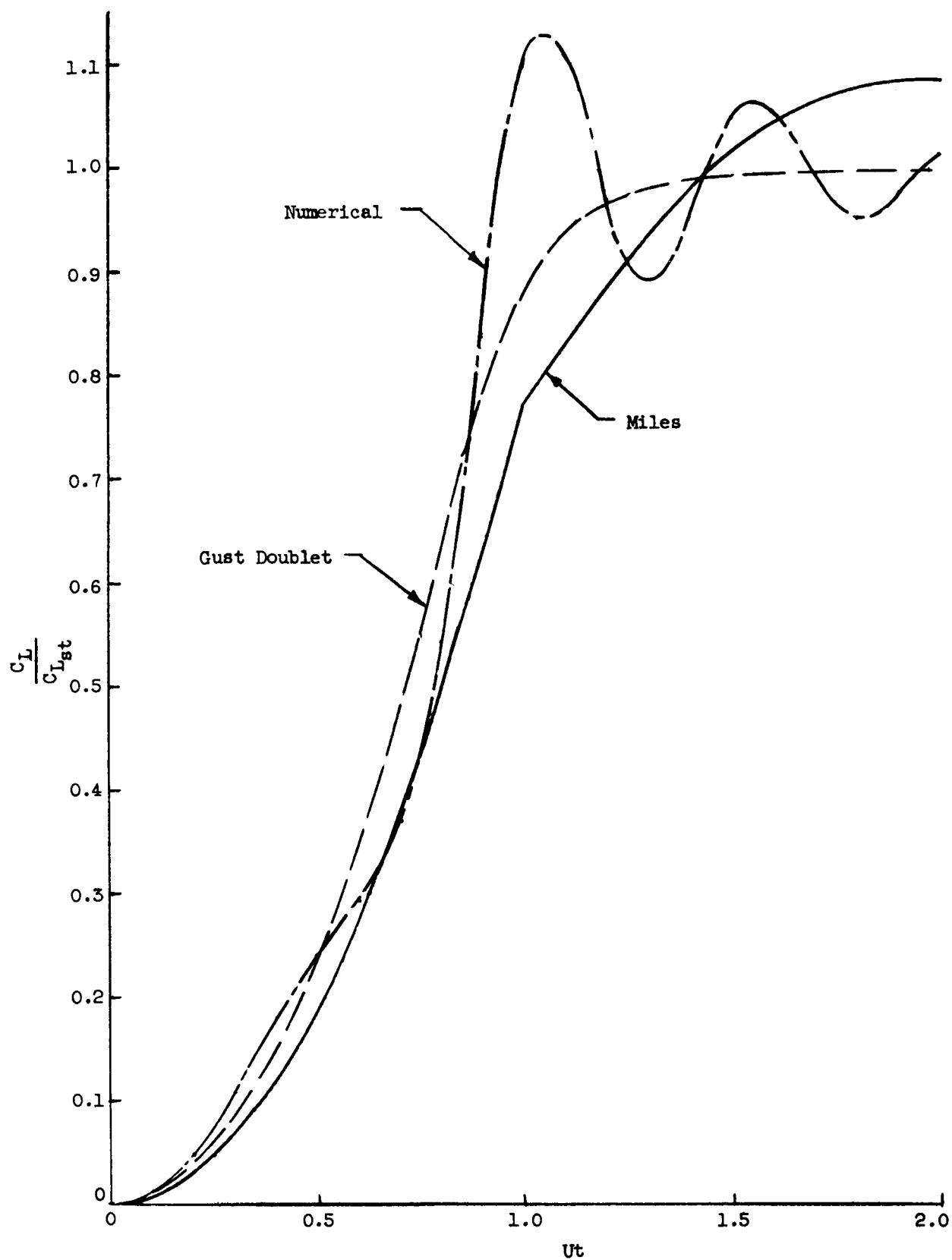


Fig. 14 - Lift Coefficient, Numerical

APPENDIX E

THE NONLINEAR PRESSURE COEFFICIENT AND RELATED COEFFICIENTS

The pressure coefficient used in Sections VII and VIII is linearized. When working with the linearized potential theory for axially symmetric bodies, it is often necessary to consider the effect of the nonlinear or quadratic terms in the pressure coefficient, in order to obtain more accurate results. This Appendix includes a derivation of these additional terms, and a few numerical results obtained with them.

The exact pressure coefficient for steady flow may be written as [27]

$$C_P = \frac{2}{\gamma M^2} \left\{ \left[1 + \frac{\gamma-1}{2} M^2 \left(1 - \frac{\bar{u}^2}{U^2} \right) \right]^{\frac{\gamma}{\gamma-1}} - 1 \right\} \quad (\text{E.1})$$

where \bar{u} is the true velocity vector. This vector has the components

$$\left. \begin{aligned} u &= U - \dot{\phi}_x \\ v &= -\dot{\phi}_r \\ w &= -\frac{1}{r} \dot{\phi}_\theta \end{aligned} \right\} \quad (\text{E.2})$$

provided the x-axis is parallel to the upstream velocity. If the expression in square brackets in (E.1) is expanded in a power series, one obtains

$$C_P = \frac{1}{U^2} \left\{ 2U\dot{\phi}_x - \dot{\phi}_r^2 - \frac{1}{r^2} \dot{\phi}_\theta^2 + \beta^2 \dot{\phi}_x^2 \right\} \quad (\text{E.3})$$

where terms of order higher than 2 in the derivatives of ϕ have been neglected. For the non-steady case, we must add the term

$$\frac{2}{U^2} \phi_t \quad . \quad (E.4)$$

Now, the potential function, ϕ , given here is the complete perturbation potential and includes the function Ψ given in Section III, the gust potential, the axial flow potential, and a steady crossflow potential, if any. The latter will be dropped from consideration in what follows since it can be looked on as a special case of the gust potential. Thus, we can write

$$\phi = \phi_a + \phi_g \cos \theta + \psi \cos \theta \quad (E.5)$$

where all θ -dependence is shown explicitly, and

$$\Psi = \psi \cos \theta \quad .$$

The subscripts a and g indicate axial and gust, respectively. A term such as ϕ_{ar} will indicate the derivative of ϕ_a with respect to r . (E.3) and (E.4) can now be combined to yield, using (E.5),

$$\begin{aligned} C_P = \frac{1}{U^2} \left\{ 2U\phi_{ax} + 2U\phi_{gx} \cos \theta + 2\phi_{gt} \cos \theta \right. \\ - \phi_{ar}^2 - (\phi_{gr} + \psi_r)^2 \cos^2 \theta - 2\phi_{ar}(\phi_{gr} + \psi_r) \cos \theta \\ - \frac{1}{r^2} (\phi_g + \psi)^2 \sin^2 \theta + \beta^2 \phi_{ax}^2 \\ \left. + \beta^2 \phi_{gx}^2 \cos^2 \theta + 2\beta^2 \phi_{ax} \phi_{gx} \cos \theta \right\} . \quad (E.6) \end{aligned}$$

The end result which is desired here is not the pressure coefficient itself, but rather the generalized force coefficient,

$$C_{F_\ell} = \frac{1}{SL^\ell} \int_0^{2\pi} \int_0^L C_P x^\ell R \cos \theta \, dx \, d\theta \quad . \quad (E.7)$$

Due to the integration on θ , the only portions of (E.6) which have a non-zero contribution to (E.7) are those terms involving $\cos \theta$. Defining that part, then, as C_P^* , yields

$$C_P^* = \frac{2 \cos \theta}{U^2} \left\{ U\phi_{gx} + \phi_{gt} - \phi_{ar}(\phi_{gr} + \psi_r) + \beta^2 \phi_{ax} \phi_{gx} \right\} \quad . \quad (E.8)$$

Inserting (E.8) into (E.7) gives

$$\begin{aligned} C_{F_\ell} = \frac{2\pi}{U^2 SL^\ell} & \left\{ \int (\phi_{gt} + U\phi_{gx}) x^\ell R(x) \, dx \right. \\ & - \int \phi_{ar} \phi_{gr} x^\ell R(x) \, dx + v_o \int \phi_{ar} x^\ell R(x) \, dx \\ & \left. + \beta^2 \int \phi_{ax} \phi_{gx} x^\ell R(x) \, dx \right\} \quad . \quad (E.9) \end{aligned}$$

The first line of (E.9) is the linear portion which has already been dealt with. The second line contains the quadratic terms which are due to radial derivatives. The third line, which is normally neglected compared to the second line, involves the axial nonlinear terms.

The remaining task, then, is to insert the Eqs. (A.4), (A.5), (8.10), (8.11), (8.12), (8.14), (8.15), and (8.16) into Eq. (E.9) and perform the required integrations. It seems best to evaluate these integrals in the same

fashion as was done in Section VIII, that is, as indefinite integrals.* However, some of the terms do not seem to be integrable in closed form, if the most general form for the integrand is used. If this is indeed the case, recourse may be had to numerical techniques.

For purposes of estimating the importance of these nonlinear terms, the case of a conical body may be considered. Here, we have $\xi_k = 0$ and only one term is required for the axial flow portion of the potential. It is also sufficient to consider only one term of the gust potential, namely, that term with $s_n = t_m = 0$. The integrals can be evaluated in this case. Line 2 of (E.9) gives, in Region B,

$$\Delta C_L = \frac{B \sqrt{1-\gamma^2}}{S U^2} \left\{ A \beta^2 \cosh^{-1}\left(\frac{1}{\gamma}\right) + \frac{A}{R'^2} \sqrt{1-\gamma^2} - 2\pi v_o \right\} \frac{x^2}{2} \quad (E.10)$$

while line 3 yields

$$\Delta C_L = - \frac{A B \beta^2 x^2}{S U^2} \sqrt{1-\gamma^2} \cosh^{-1}\left(\frac{1}{\gamma}\right) \quad (E.11)$$

* The limits of integration to be used are slightly more involved than those given in Table I. The location of the Mach line emanating from ξ_k (axial flow source distribution origin) relative to the other regions must be considered. In addition, the second integrand in line 2 of (E.9) actually involves the unit step function, $H(Ut-x)$, which will, in some cases, alter the integration.

For Regions C and D, line 2,

$$\begin{aligned}
 \Delta C_L = & \frac{AB\sqrt{1-\gamma^2}}{4SU^2} \left\{ \frac{\gamma^2 Ut(1+R'^2) - (1-\gamma^2) [x(1+R'^2) + Ut(1-2R'^2)]}{R'^2(1+R'^2)^2} \sqrt{Z} \right. \\
 & + \frac{M^2 U^2 t^2 (1-2R'^2)}{(1+R'^2)^{5/2}} \sinh^{-1} \bar{Z} + \frac{2U^2 t^2 (2x-Ut)}{(1+R'^2) \sqrt{Z}} \\
 & + x^2 \left[-M + \beta^2 \cosh^{-1} \left(\frac{1}{\gamma} \right) + \frac{1}{R'^2} \sqrt{1-\gamma^2} \right. \\
 & \left. \left. + \beta^2 \log \left(\frac{(M+1) [\sqrt{X} + (x-Ut)]}{\gamma x} \right) \right] \right\} \\
 & - \frac{\pi B v_0 x^2 \sqrt{1-\gamma^2}}{SU^2}
 \end{aligned} \tag{E.12}$$

and for line 3,

$$\begin{aligned}
\Delta C_L = & \frac{AB\beta^2 \cosh^{-1}\left(\frac{1}{\gamma}\right)}{2SU^2} \left\{ -x^2 \sqrt{1-\gamma^2} \right. \\
& + \frac{M^2 R'^2 U^2 t^2 (R'^2 - 2)}{2(1+R'^2)^{5/2}} \sinh^{-1} \bar{Z} \\
& + \frac{1}{2(1+R'^2)^2 \sqrt{Z}} \left[-3U^2 t^2 R'^2 (x(1-R'^2) - Ut) \right. \\
& + x(1+R'^2)^2 (R'^2 x^2 + 4Utx - 4U^2 t^2) \\
& + Ut(1+R'^2)(R'^2 x^2 - 2Utx + 2U^2 t^2) \\
& + \frac{\sqrt{Z}}{2(1+R'^2)^2} \left[-Ut(2+8R'^2+3\gamma^2) \right. \\
& \left. \left. + x(1+R'^2)(2-\gamma^2) \right] \right\} .
\end{aligned} \tag{E.13}$$

In Eqs. (E.10) and (E.13) the following special abbreviations were used:

$$A = \frac{2\pi v_o / \beta^2}{\cosh^{-1}\left(\frac{1}{\gamma}\right) + \frac{1+2\gamma^2/\beta^2}{\gamma^2} \sqrt{1-\gamma^2}} \quad (E.14)$$

$$B = \frac{-U}{\cosh^{-1}\left(\frac{1}{\gamma}\right) + \frac{\beta^2}{\gamma^2} \sqrt{1-\gamma^2}} \quad (E.15)$$

$$Z = (x-Ut)^2 + R'^2 x^2 \quad (E.16)$$

$$\bar{Z} = \frac{x-Ut + R'^2 x}{R'Ut} \quad (E.17)$$

The moment and bending coefficients can also be found, although the lift coefficient is sufficient for the purpose of ascertaining the effect of the nonlinear terms.

The steady-state solutions are shown in Figs. 15 and 16. It is clear that, to obtain accurate results, the nonlinear terms must be included in the expressions for force coefficients. The curves labeled nonlinear contain all three lines of Eq. (E.9). The third line, which is often neglected in comparison to the second line, is important unless the Mach number is close to one. The nonlinear terms are more important for blunter cones, as is to be expected.

A cursory examination of the exact solutions of the nonlinear steady fluid flow equations for yawed cones indicates that the inclusion of the quadratic terms gives a slight overestimate of the lift coefficient. More detailed comparisons should be made to facilitate estimates of accuracy and applicability of this theory.

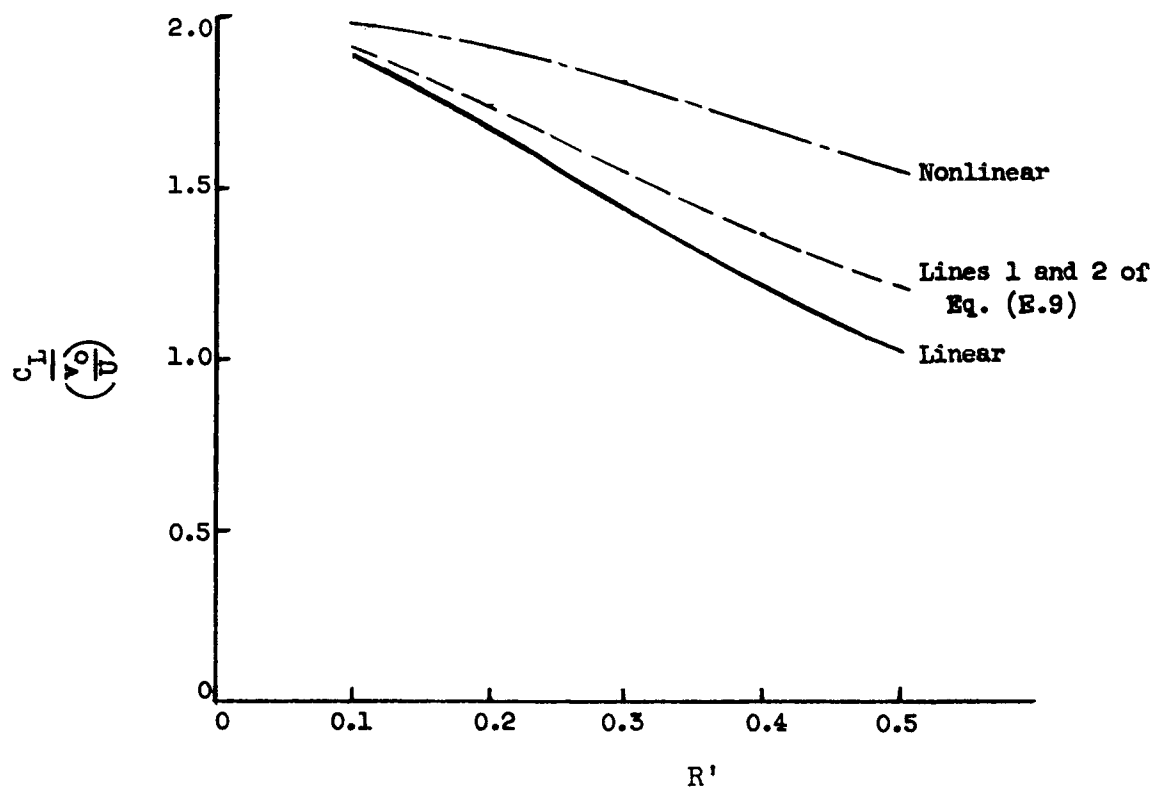


Fig. 15 - Steady-State Lift Coefficient for $M = 1.5$ (Nonlinear)

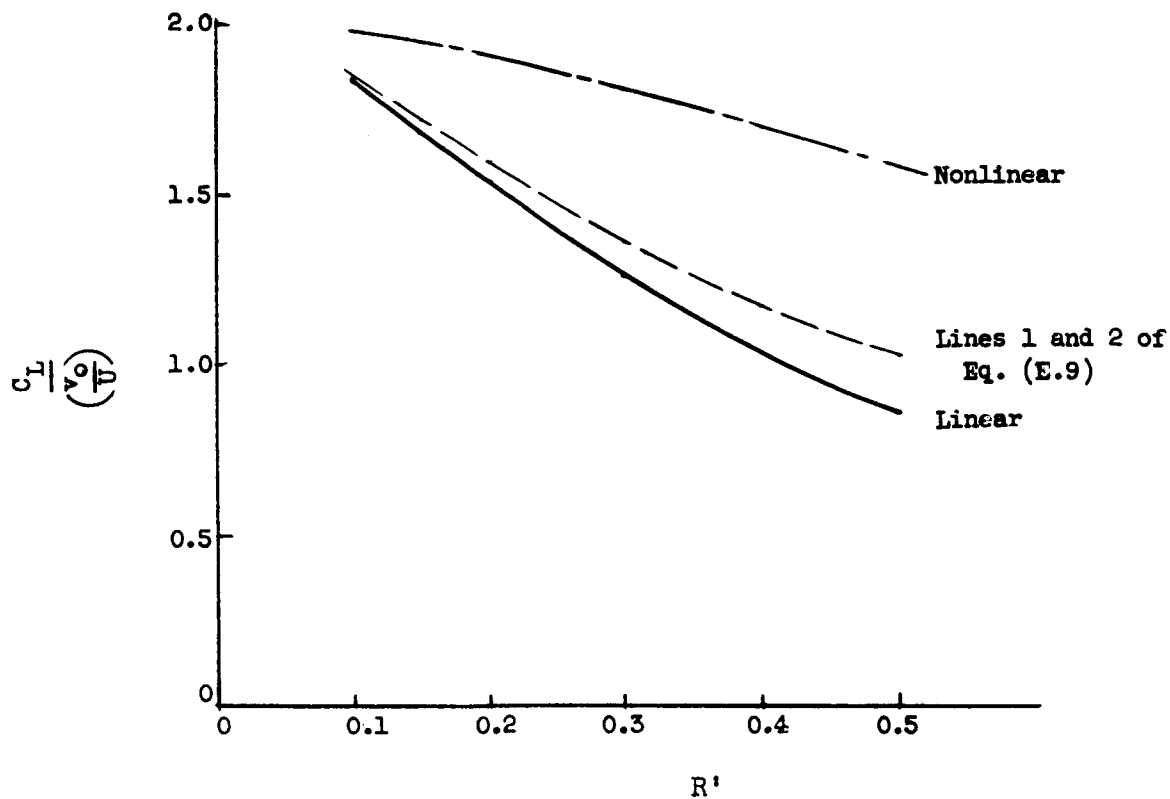


Fig. 16 - Steady-State Lift Coefficient for $M = 2.0$ (Nonlinear)

Figure 17 shows the effect of the nonlinear terms on the growth of lift for a cone of unit length. The initial rate of growth is decreased somewhat, although it is still greater than that of Miles. The "knee" at $Ut = 1$ is due to the step function occurring in the second term of line 2. It is recalled that this term arose from the potential Ψ given in Section III.

The nonlinear terms do not affect the growth of lift as much as they affect the final steady-state value of the lift coefficient. It might be useful, as an approximation, to use the linear growth of lift curve, but modified in magnitude to give the nonlinear steady value. The linear curve is much easier to evaluate than the nonlinear.

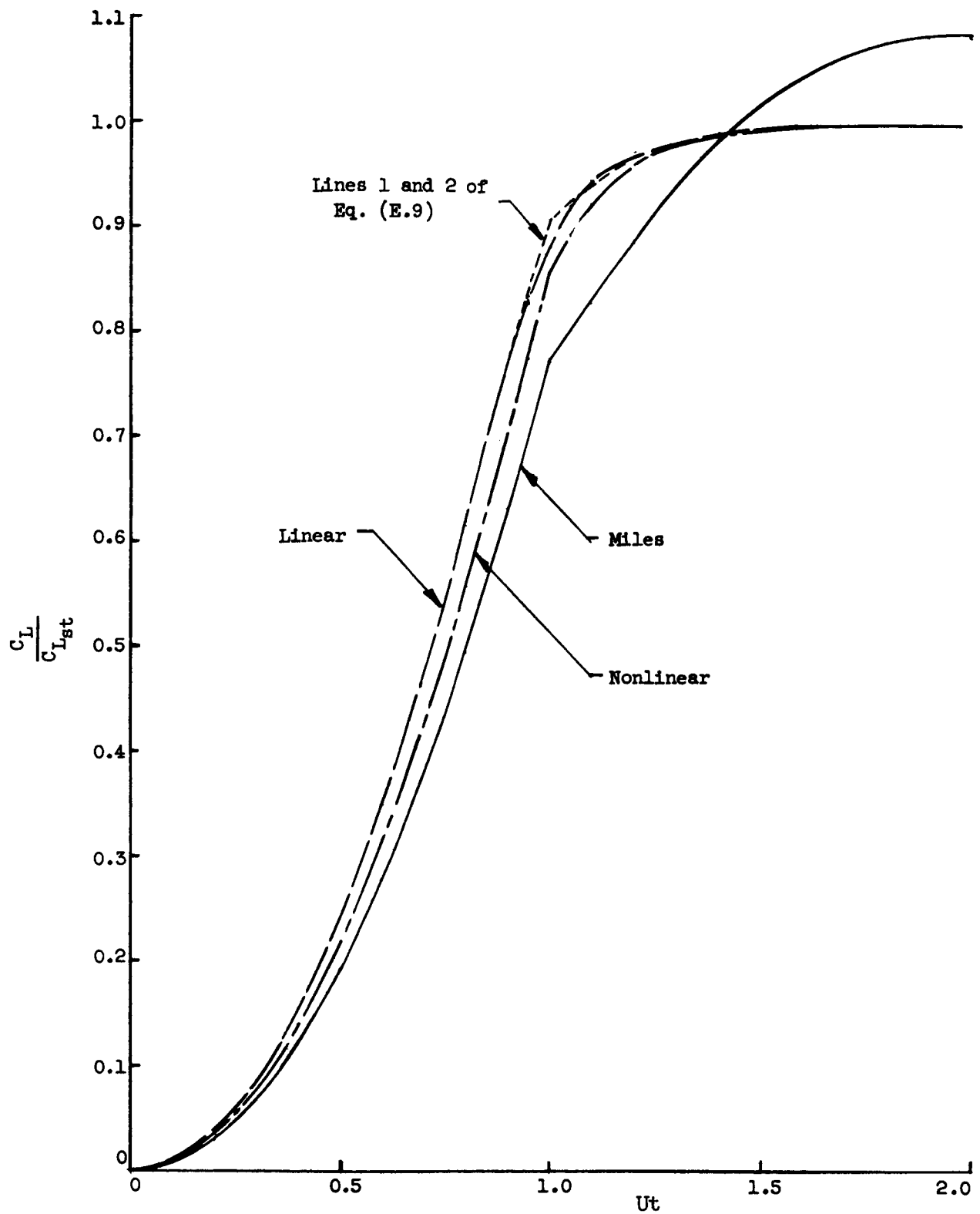


Fig. 17 - Growth of Lift for $M = 2.0$, $R' = 0.15$ (Nonlinear)